pancreatic alpha cells and stored in secretory vesicles [24]. Moreover, it has also been shown that TTR co-localized with glucagon exactly in pancreatic alpha cells, suggesting that TTR synthesized by pancreatic alpha cells may be involved in glucose homeostasis [24]. However, the biological significances of TTR expressed in pancreatic alpha cells remain unknown.

In view of the evidences provided in previous reports, we hypothesized that TTR may play important roles in glucose homeostasis. In this study, we focused on TTR that is synthesized by pancreatic alpha cells, and we evaluated the possible role of TTR in expression and plasma levels of glucagon during glucose fluctuations.

2. Materials and methods

2.1. Animals

Wild-type (WT) and TTR knockout (TTR KO) mice in the C57BL/6 J background [28], were used in this study. Mice were adult males, each 8–10 weeks old and each weighing 20–25 g. The animals were maintained in a pathogen-free environment at the Center for Animal Resources and Development, Kumamoto University.

2.2. Insulin tolerance test (ITT)

In the ITT, performed after a 3-h fast, human regular insulin (1 IU/kg) was administered intraperitoneally (i.p.) to mice, and the blood glucose level was measured by using an Accu-Chek Inform Blood Glucose Monitoring System (Roche Diagnostics, Indianapolis, IN).

2.3. Fasting conditions and collection of samples

Plasma samples of mice for ELISA were collected at 0, 6, 12, and 24 h after fast. Samples of pancreas and liver for (qRT-PCR) were sharply excised, and then immediately frozen in liquid nitrogen.

2.4. Cells and cell culture

The cell lines PANC-1 (human pancreas epithelioid carcinoma cells), alpha TC1 clone 6 (mouse pancreatic alpha cells), and HepG2 (human hepatocellular carcinoma cells) were obtained from ATCC (Manassas, VA) and were cultured in DMEM (Invitrogen, Grand Island, NY) supplemented with 10% FBS. All cells were grown in 5% CO_2 at 37 °C.

2.5. RNA isolation and qRT-PCR

Total RNA was isolated from each tissue specimen and treated cells by using TRIzol (Invitrogen, Carlsbad, CA), according to the manufacturer's protocol. Total RNA (0.5 μg) was reverse-transcribed to cDNA by using the ExScript RT reagent (Takara Bio Inc., Shiga, Japan) according to the manufacturer's instructions. Each PCR reaction was done with 2 μl of cDNA and 0.2 μM of each primer in a LightCycler System with SYBR Premix Ex Taq (Takara Bio Inc.). Agarose gel electrophoresis was also performed as previously described. The following primers were used: mouse glucagon: forward, 5-TGAATTTGAGAGGCATGCTG-3; reverse, 5-GGTTTGAATCAGCCAGTTGA-3; mouse TTR: forward, 5-CATGAAT TCGCGGATGTG-3; reverse, 5-GATGGTGTAGTGGCGATGG-3; mouse β-actin: forward, 5-TGACAGGATGCAGAAGGAGA-3; reverse, 5-GC TGGAAGGTGGACAGTGAG-3; human TTR: forward, 5-CATTCTTG GCAGGATGGCTTC-3; reverse, 5-CTCCCAGGTGTCATCAGCAG-3; and human glyceraldehyde-3-phosphate dehydrogenase (GAPDH): forward, 5-GCACCGTCAAGGCTGAGAAC-3; reverse, 5-ATGGTGGTG AAGACGCCAGT-3.

2.6. Transfection and fasting in vitro

Cells were cultured in 12 well culture plates (Becton, Dickinson, Franklin Lakes, NJ) at a density of 2×10^5 cells per well, at 37 °C in a humidified atmosphere of 5% CO_2 in air for 48 h. Confluent alpha TC1 clone 6 cells were transfected with two different kinds of siRNA against murine TTR, and PANC-1 cells were transfected with human TTR plasmid by using Lipofectamine 2000 (Invitrogen) according to the manufacturer's protocol. After incubation for 24 or 48 h in serum-free medium, total RNA and protein were isolated. Alpha TC1 clone 6 cells or PANC-1 cells transiently transfected with control siRNA or control vector were used as controls. Chemical siRNA sequences for TTR siRNA1 were as follows: TTR siRNA1 sense strand 5′-CAGUGUUCUUGCUCUAUAATT-3′, TTR siRNA1 antisense strand 5′-UUAUAGAGCAAGAACACUGTT-3′ (Sigma–Aldrich, Tokyo, Japan). For evaluation of the effect of fasting on cells, after cells were incubated in serum-free high-glucose or low-glucose DMEM for 72 h, and thereafter total RNA was isolated.

2.7. Protein extraction form pancreas and pancreatic islets

Protein in the total pancreas and isolated pancreatic islets from mice was obtained by using acid ethanol (15% 1 M HCl, 75% ethanol, 10% H_2O).

2.8. Isolation of pancreatic islets

Mouse pancreatic islets were isolated by means of collagenase digestion. Mice were anesthetized by i.p. with sodium thiopental. Collagenase (collagenase type S-1, 0.6 mg/ml; Nitta Gelatin Inc., Osaka, Japan) was dissolved in Hanks' Balanced Salt Solutions (Sigma–Aldrich) with 800 KIU/ml aprotinin (Wako, Osaka, Japan). The collagenase solution was injected into the common bile duct. Pancreas were dissected and incubated in the collagenase solution at 37 °C for 20 min with shaking. These samples were then mixed with ice-cold isotonic sucrose buffer and were chilled on ice for 20 min. Clarified islets were collected for use in experiments.

2.9. Analysis of glucagon secretion

After being incubated in DMEM for 24 h, 5 groups, for each group contained 15 islets, were incubated for 1 h in Ca^{2+}-containing HEPES-added Krebs–Ringer bicarbonate buffer (HKRB) with 2.2 mM glucose in 5% CO_2 at 37 °C, followed by test incubation for 1 h in HKRB with 2.2 or 22 mM glucose.

2.10. Immunohistochemical staining

Paraffin-embedded 4-μm-thick sections were prepared and deparaffinized in xylene and rehydrated in graded alcohols. Slides were treated with periodic acid for 10 min at room temperature, after which they were incubated in 5% normal serum for 1 h at room temperature in a moist chamber. For immunohistochemical staining of glucagon, a polyclonal rabbit anti-glucagon antibody (Cell Signaling Technology, Danvers, MA), diluted 1:100 in dilution buffer, served as the primary antibody. Rabbit anti-mouse TTR antiserum, diluted 1:50 in dilution buffer, served as the primary antibody for mouse TTR. The secondary antibody was an HRP-conjugated goat anti-rabbit immunoglobulin antibody (Dako, Glostrup, Denmark) diluted 1:100 in buffer. The dilution buffer was 0.5% Bovine serum albumin (BSA). Reactivity was visualized via the DAB Liquid System (Dako), according to the manufacturer's instructions. Sections were counterstained with hematoxylin.

2.11. ELISA

The glucagon concentration in plasma, extracts of total pancreas and islets from mice, and cell lines was measured by using the Rat Glucagon ELISA Kit (Wako), according to the manufacturer's instructions for undiluted plasma samples, 1000 times dilution of extracts of pancreas and islets, 500 times dilution of cell supernatants, and 50 times dilution of cell lysates.

2.12. Statistics

Data were expressed as means ± S.D. and ±S.E.M., according to the previous study [29]. Controls and treated groups were compared by using Student's *t* test. The accepted level of significance was $P < 0.05$.

3. Results

3.1. Change in blood glucose levels in WT and TTR KO mice during the ITT

RT-PCR confirmed expression of TTR mRNA in the pancreas of mice (Fig. 1A). In sections of pancreatic tissues, TTR was expressed in all islets from WT mice, with cells showing a preferential peripheral distribution, but islets from TTR KO mice evidenced no TTR expression (Fig. 1A). ITT showed that the blood glucose level in WT mice started to recover at 30 min after the insulin injection (Fig. 1B). However, those in TTR KO mice decreased sharply by 60 min after the injection compared with the baseline of the blood glucose level. Furthermore, TTR KO mice had continuously suppressed blood glucose levels compared with WT mice at 60, 90, 120, and 180 min after the insulin injection (Fig. 1B). We assumed that the impaired plasma glucagon levels caused the sharp decrease of the blood glucose levels in the ITT.

3.2. Plasma glucagon levels in WT and TTR KO mice in the ITT and during fasting

We next investigated plasma glucagon levels in WT and TTR KO mice. As Fig. 2A shows, although WT mice showed higher plasma glucagon levels after the insulin injection, TTR KO mice showed a much smaller increase in plasma glucagon levels in a time-dependent manner after the injection. In addition, in sections of pancreatic tissues from WT and TTR KO mice at 20 min after the insulin injection, almost all of the islets from WT mice demonstrated strong glucagon immunoreactivity, but islets from TTR KO mice showed only weak immunoreactivity (Fig. 2B). Furthermore, we compared plasma glucagon levels between WT and TTR KO mice during chronic glucose fluctuations induced by fasting. As seen in Fig. 2C, consistent with the results of the ITT, TTR KO mice showed significantly lower plasma glucagon level by fasting. In contrast to the glucagon levels, no significant difference of plasma insulin levels between WT and TTR KO mice was observed (Fig. S1).

3.3. Glucagon content in pancreatic islets from WT and TTR KO mice

We next determined the glucagon content in pancreatic islets from WT and TTR KO mice. Under normal conditions, pancreatic islets from WT mice demonstrated a strong positive immunoreactivity for glucagon, with a preferential distribution in the periphery (Fig. 3A). Pancreatic islets from TTR KO mice, however, showed a much weaker positive reaction (Fig. 3A). The quantitative analysis showed that in TTR KO mice, the glucagon content in the total pancreas was significantly lower than that for WT mice, *i.e.*, about 10% of the glucagon content of WT mice (Fig. 3B). To confirm these results, pure pancreatic islets were isolated and analyzed. As seen in Fig. 3C, similar to the results for the total pancreas, the glucagon content in islets isolated from TTR KO mice was about 50% of that in from WT mice.

3.4. Glucagon secretion from pancreatic islets isolated from TTR KO mice

To confirm the results obtained from *in vivo* experiments, glucagon secretion from pure pancreatic islets-isolated from WT and TTR KO mice were analyzed. Transfer from high-glucose condition to low-glucose condition has been shown to induce glucagon secretion from pancreatic islets. In our study, performed under similar conditions, pancreatic islets from WT mice showed

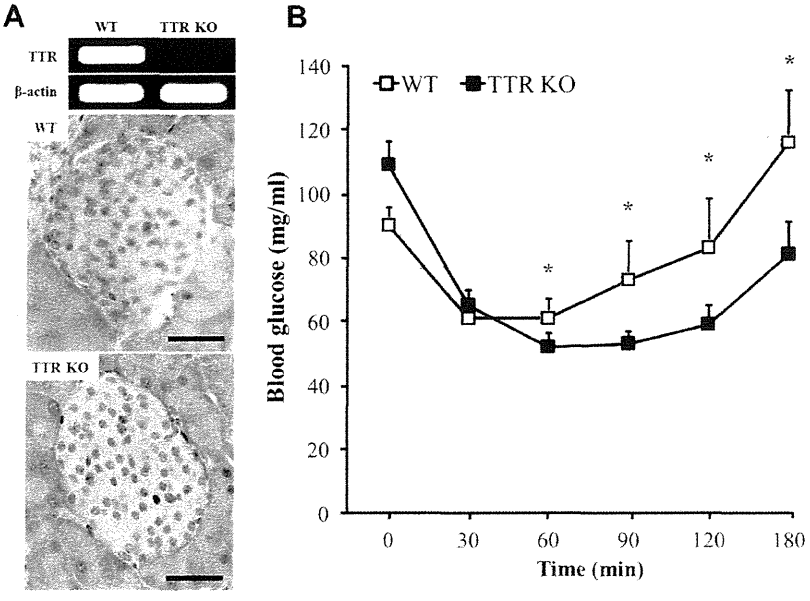

Fig. 1. TTR expression in pancreatic tissues of mice and changes in blood glucose levels in WT and TTR KO mice during the ITT. (A) Expression of TTR mRNA in the pancreas of mice (top panel); TTR expression in islets from WT mice, with cells showing a preferential peripheral distribution (middle panel), but no TTR expression in TTR KO mice (bottom panel). Scale bars = 100 μm. (B) Mice received human regular insulin (1 IU/kg i.p.), and the serum glucose level was monitored at 0, 30, 60, 90, 120, and 180 min (mean ± S.E.M.). $n = 6$. $^*P < 0.05$.

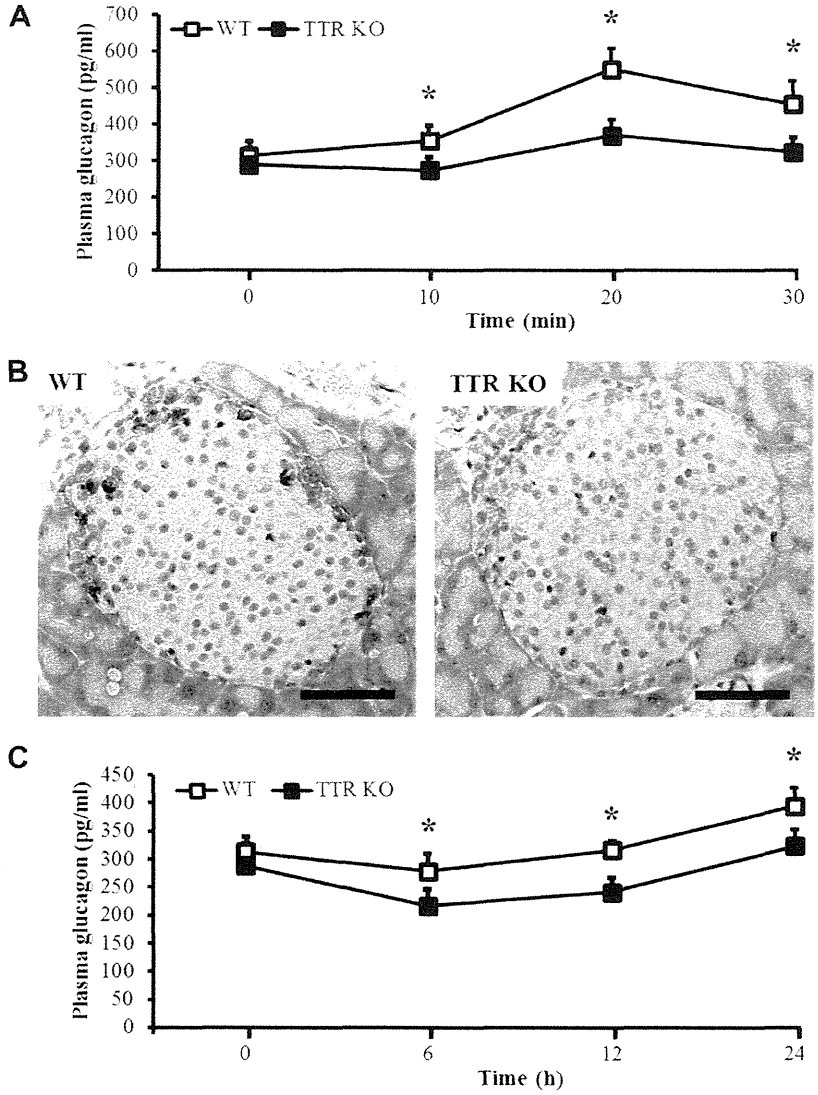

Fig. 2. Plasma glucagon levels in WT and TTR KO mice in the ITT and during fasting. (A) Mice underwent the ITT, and plasma glucagon was measured at 0, 10, 20, and 30 min by using ELISA (mean ± S.E.M.). $n = 10$. (B) Examples of pancreatic islets from mice after the ITT. At 20 min after ITT, immunohistochemistry revealed high-intensity glucagon staining in pancreatic islets from WT mice (left) and low-intensity glucagon staining in pancreatic islets from TTR KO mice (right). Scale bars = 100 μm. (C) Mice were fasted for 24 h, and plasma glucagon was measured by ELISA at 0, 6, 12, and 24 h (mean ± S.E.M.). $n = 11$. $^*P < 0.05$.

increased glucagon secretion in the low-glucose compared with the high-glucose condition. In addition, islets from TTR KO mice had glucagon levels similar to those of WT mice in the high-glucose condition. However, no increase in glucagon level was observed in the islets from TTR KO mice in response to the low-glucose condition, in contrast to WT mice. The glucagon levels in the islets from TTR KO mice were significantly lower than those from WT mice under low-glucose conditions (Fig. 4A). We also evaluated the glucagon contents remaining in pancreatic islets after glucagon secretion. Pancreatic islets from TTR KO mice showed a significantly lower level of glucagon than islets from WT mice-only about 40% of the WT level (Fig. 4B). Because the TTR KO islets showed the lower glucagon content, we assumed that the content of glucagon was impacted by the decrease of glucagon expression.

3.5. Changes in glucagon expression as related to TTR expression

We next determined glucagon mRNA levels after 12 h of fasting. Expression of glucagon mRNA in the total pancreas from TTR KO mice was significantly lower than that from WT mice (Fig. 5A). While, no obvious alteration was seen in insulin mRNA expression (Fig. S2). In addition, downregulation of TTR expression by two different sequences of TTR siRNA led to a significant reduction in glucagon expression in alpha TC1 clone 6 cells at both mRNA andprotein levels (Fig. 5B, Figs. S3 and S4). In contrast, overexpression of WT-TTR by using the TTR plasmid significantly increased glucagon mRNA expression in PANC-1 cells (Fig. 5C).

3.6. Starvation-induced changes in pancreatic TTR expression

Previous reports demonstrated that TTR levels decreased during progressive malnutrition and that this effect was linked to expression of TTR in the liver, the main organ of production of TTR circulating in the blood [17]. In our study, as expected, expression of TTR in the liver from WT mice significantly decreased. In contrast, expression of TTR in the total pancreas from WT mice markedly increased, about 2.5 times, during starvation induced by fasting for 24 h (Fig. 6a and b). Similar to the results obtained from *in vivo* experiments, HepG2 cells, a liver cell line, showed a marked reduction in TTR expression after incubation under low-glucose

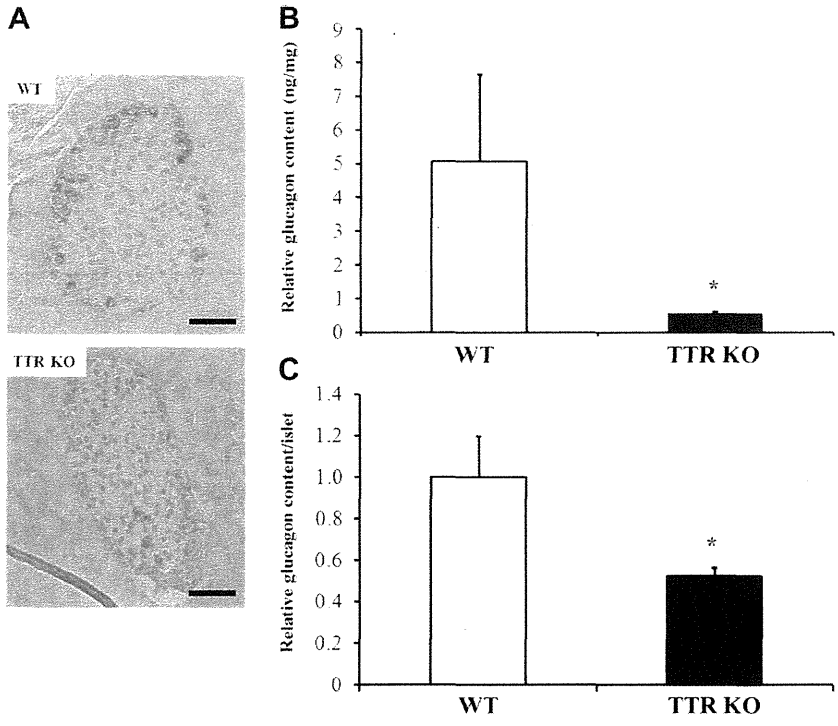

Fig. 3. Glucagon content in pancreatic islets from WT and TTR KO mice. (A) An example of high-intensity glucagon staining in pancreatic islets from WT mice (top) and low-intensity glucagon staining in pancreatic islets from TTR KO mice (bottom). Scale bars = 100 μm. (B) Glucagon content in the total pancreas from WT and TTR KO mice as measured by ELISA (mean ± S.D.). $n = 6$. (C) Glucagon content in isolated pancreatic islets from WT and TTR KO mice, as measured by ELISA (mean ± S.D.). $n = 3$. $^{*}P < 0.05$.

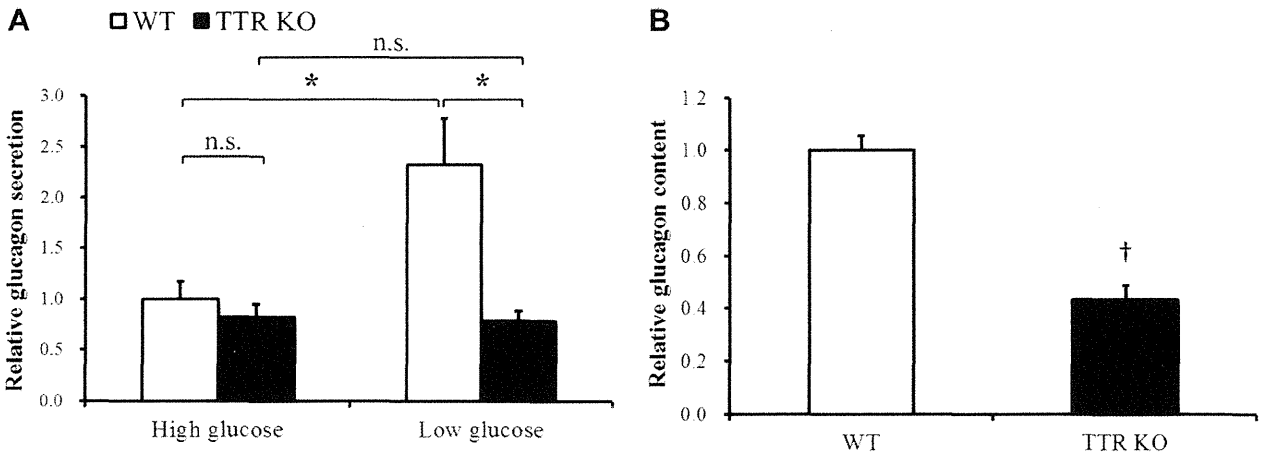

Fig. 4. Glucagon secretion from pancreatic islets from WT and TTR KO mice. (A) Pancreatic islets isolated from WT and TTR KO mice were incubated under high- (22 mM) or low- (2.2 mM) glucose condition. Glucagon levels were assessed by ELISA (mean ± S.E.M.). $n = 5$. $^{*}P < 0.05$. n.s., not significant. (B) Remaining glucagon contents in isolated pancreatic islets from WT and TTR KO mice after glucagon secretion after incubation in low-glucose condition, as measured by ELISA (mean ± S.E.M.). $n = 5$. $^{\dagger}P < 0.01$.

conditions for 72 h. However, alpha TC1 clone 6 cells evidenced significantly increased glucagon mRNA expression after incubation in glucose-poor medium for 48 h (Fig. 6c and d).

4. Discussion

A previous report suggests that, on the basis of electron microscopic evidence, TTR in pancreatic islets is mainly expressed in pancreatic alpha cells and is stored in secretory vesicles [24]. In the present study, we demonstrated that TTR KO mice, compared with WT mice, evidenced impaired blood glucose recovery and plasma glucagon levels during both acute and chronic glucose fluctuations. These results were confirmed by using isolated pancreatic islets from WT and TTR KO mice. These interesting phenomena suggest that TTR plays important roles in glucose homeostasis during glucose fluctuations, especially periods of low blood glucose levels, by regulating the amount of glucagon secreted.

One interesting finding of this study is that the lack of TTR reduced the plasma glucagon level during both acute and chronic glucose fluctuations. Glucagon and insulin constitute part of a feedback system that keeps blood glucose levels stable. The reduced glucagon level destroys the balance between insulin and glucagon, and affects the stability of blood glucose levels. These effects may be amplified by injections of insulin used to treat insulin-dependent diabetes, or by long periods of malnutrition. The pancreas releases glucagon when blood glucose levels fall too low,

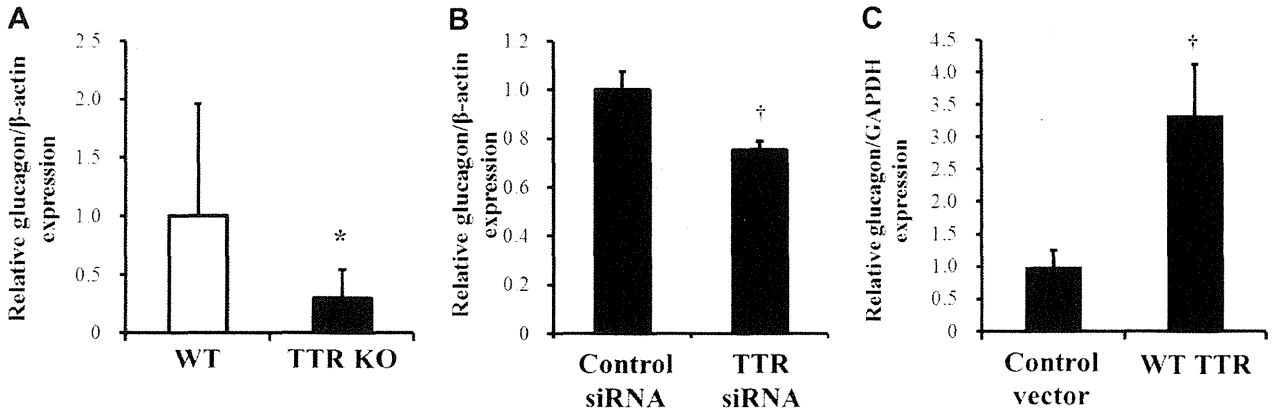

Fig. 5. Effects of TTR on glucagon expression. (A) Mice were fasted for 12 h, and glucagon mRNA expression was measured by means of qRT-PCR (mean ± S.D.). $n = 14$. (B) effect of blocking TTR signaling on glucagon mRNA expression in alpha TC1 clone 6 cells. Blocking was achieved by using TTR siRNA (100 nM) (mean ± S.D.). $n = 3$. (C) Effect of TTR overexpression on glucagon mRNA expression in PANC-1 cells. Overexpression was achieved by using TTR plasmid (0.3 μg) (mean ± S.D.). $n = 3$. $^{*}P < 0.05$; $^{\dagger}P < 0.01$.

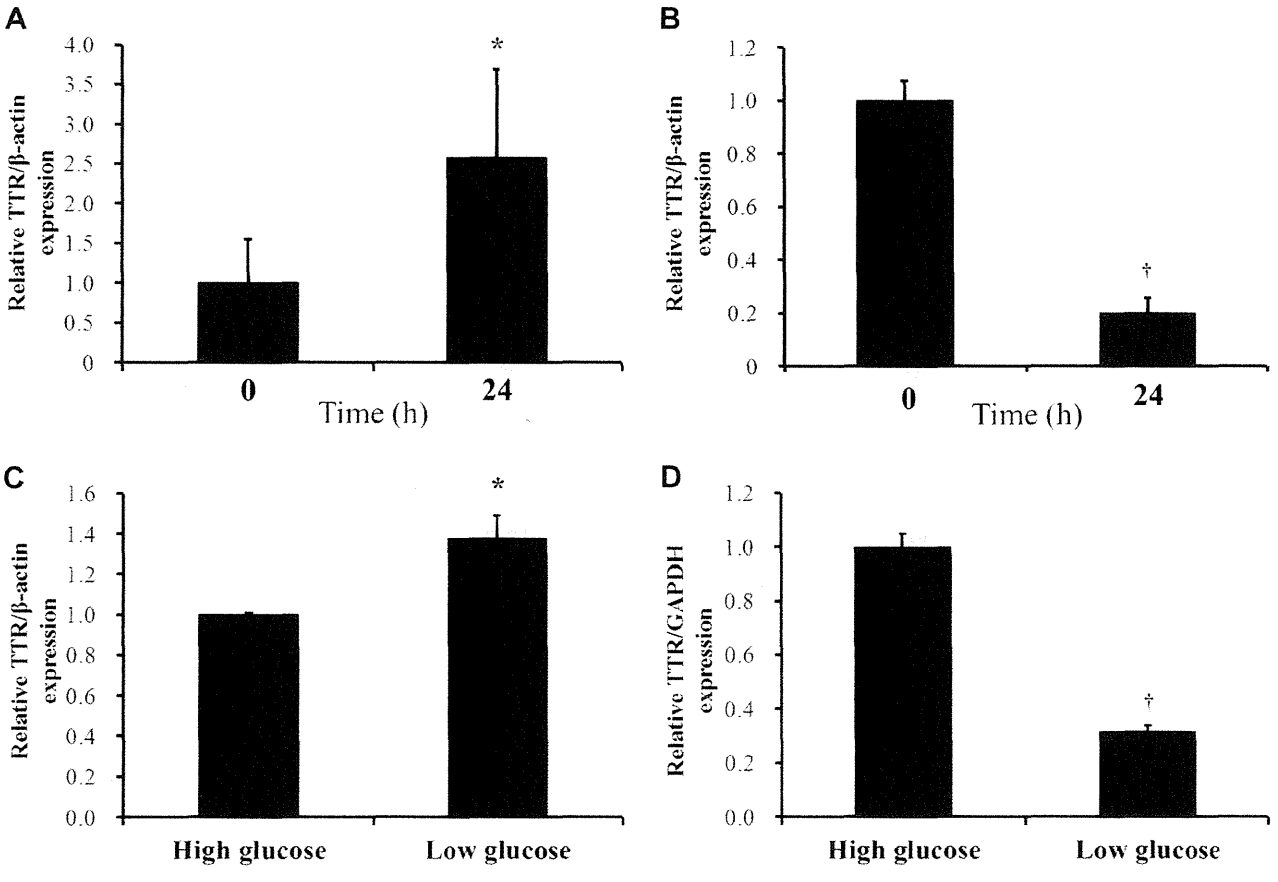

Fig. 6. Effects of starvation on TTR expression in pancreas and liver. WT mice were fasted for 24 h, and TTR mRNA expression in pancreas (A) and liver (B) was measured by means of qRT-PCR (mean ± S.D.). (C) and (D) alpha TC1 clone 6 (C) or HepG2 (D) cells were incubated under high- or low-glucose condition for 72 h. TTR mRNA expression was measured by means of qRT-PCR (mean ± S.D.). $n = 3$. $^{*}P < 0.05$; $^{\dagger}P < 0.01$.

and glucagon facilitates the liver's conversion of stored glycogen into glucose, which is released into the bloodstream. Low plasma glucagon levels cause a failure in the relief of acute or chronic severe hypoglycemia, which affects many important organs and major physiological functions [6]. Especially, because neurons cannot use other energy sources such as fatty acids to any great degree, brain depends absolutely on glucose as a fuel [30]. Thus, rapid response and dynamic glucagon secretion when blood glucose levels are low is extremely important for maintenance of glucose homeostasis. Our data suggest that TTR performs a novel function and plays important roles in stabilizing blood glucose levels via control of glucagon. It should be noted that, despite the well-known fact that glucagon concentration is regulated by insulin concentration, no obvious difference in plasma insulin levels was observed between WT and TTR KO mice (Fig. S1). These data suggest that TTR in pancreatic alpha cells played an important role to increase

the plasma glucagon levels during glucose fluctuations. A conditional TTR KO mouse which lack TTR only in pancreas may help confirming these findings. Our future studies will focus on more precise determination of the roles of TTR in glucose homeostasis.

In the present study, we found that TTR KO mice showed a significantly lower glucagon content compared with WT mice, and we found a similar phenomenon in the *in vitro* studies using pancreatic islets. It should be noticed that the similar numbers of pancreatic islets in whole pancreas of WT and TTR KO mice were observed by microscope (average number of WT: 32 ± 6/field; TTR KO: 28 ± 4/field). Moreover, we found that glucagon mRNA expression in pancreatic cell lines had a high positive association with the level of TTR expression. These results suggest that the lack of TTR impaired the accumulation or storage of glucagon in pancreatic alpha cells, and we considered that the reduced contents of glucagon could be caused by the decrease of mRNA levels. As shown in Figs. 1 and 2, by ITT, plasma glucagon levels 20 min post-injection were lower in TTR KO than WT, and significant differences were noted from 60 min in blood glucose level. These results suggest that because pancreatic alpha cells rapidly secrete abundant glucagon in response to hypoglycemia, and since the half-life of glucagon is relatively short, 5–6 min [4], the lack of TTR may reduce the level of glucagon mRNA, which in turn leads to the deficiency of plasma glucagon levels for insulin antagonistic activity. Although the role of TTR in glycogenolysis in liver has yet to be determined, TTR may serve as one of the enhancers of glucagon expression after acute secretion of glucagon in pancreatic alpha cells. Also, we previously reported that glucose metabolism is impaired in familial amyloidotic polyneuropathy, which is caused by mutated TTR, in which amyloid deposition commonly occurs in the pancreas [31]. Previous reports demonstrated that glucagon gene expression is tightly controlled by various transcription factors, such as Pax6, Foxa1, Foxa2, and MafB/cMaf [2,32,33]. Of these transcription factors, Foxa2 (also called hepatic nuclear factor-3) is known to be essential for strong expression of TTR gene in the liver [34,35]. It should be noted that Pax6 mRNA expression was significantly reduced by TTR knockdown with siRNA in alpha TC1 clone 6 cells (Fig. S5). These lines of evidence suggest that TTR in pancreatic alpha cells may also be controlled by various transcription factors, such as Pax6 and Foxa2, in response to hypoglycemia and may serve as a mediator of up-regulation of glucagon expression. In addition to the glucagon contents, because TTR is stored in secretory vesicles [24], TTR may affect the secretion of glucagon. Moreover, since we also found that the expression levels of insulin was also affected, but not obviously, by the lack of TTR (Fig. S2), further investigation is needed to explain in detail the mechanism underlying cross-talk between glucagon and TTR expression in glucose homeostasis. In addition, instead of normal cells, we used alpha TC1 clone6 and PANC-1 cell lines to obtain supportive evidence (Figs. 5 and 6). Unlike normal pancreatic alpha cells, alpha TC1 clone 6 cells express the high levels of glucagon by the control of the rat preproglucagon promoter and terminally differentiated. PANC-1 is an epithelioid carcinoma cell line derived from human pancreas and secret the low levels of hormones. Our future studies will focus on more precise determination by using the normal pancreatic alpha cells of the roles of TTR in glucose.

Other interesting findings of this study are that, different from the situation in the liver, hypoglycemia that was induced by insulin injections and fasting significantly enhanced TTR expression in pancreatic alpha cells, and starvation produced a similar result. These findings suggest that TTR expression may be controlled by specific transcriptional regulation in pancreatic alpha cells as described above, which differ from hepatic cells. We will clarify the mechanism in the future study.

In conclusion, unlike liver that synthesize TTR, the pancreas expresses TTR by means of a distinct mechanism. In addition to the well-known function of TTR, such as transporting thyroxine in association with retinol-binding protein, TTR that is expressed in pancreatic alpha cells may play important roles in glucose homeostasis during glucose fluctuations by regulating glucagon expression.

Acknowledgments

The authors thank Hiroko Katsura for technical assistance. This work was supported in part by the Advanced Education Program for Integrated Clinical, Basic and Social Medicine, Graduate School of Medical Sciences, Kumamoto University (Program for Enhancing Systematic Education in Graduate Schools, MEXT, Japan). The authors' work was supported by grants from the Amyloidosis Research Committee; the Pathogenesis, Therapy of Hereditary Neuropathy Research Committee; the Surveys and Research on Specific Diseases from the Ministry of Health and Welfare of Japan; and Research for the Future Program Grant and Grants-in-Aid for Scientific Research (B) 20253742 from the Ministry of Education, Science, Sports and Culture of Japan. This work was also supported in part by the scholarship for the Graduate School of Medical Sciences, Kumamoto University, Japan.

Appendix A. Supplementary data

Supplementary data associated with this article can be found, in the online version, at http://dx.doi.org/10.1016/j.febslet.2012.10.025.

References

[1] Dunning, B.E. and Gerich, J.E. (2007) The role of alpha-cell dysregulation in fasting and postprandial hyperglycemia in type 2 diabetes and therapeutic implications. Endocr. Rev. 28, 253–283.
[2] Gromada, J., Franklin, I. and Wollheim, C.B. (2007) Alpha-cells of the endocrine pancreas: 35 years of research but the enigma remains. Endocr. Rev. 28, 84–116.
[3] Jiang, G. and Zhang, B.B. (2003) Glucagon and regulation of glucose metabolism. Am. J. Physiol. Endocrinol. Metab. 284, 671–678.
[4] Alford, F.P., Bloom, S.R. and Nabarro, J.D. (1976) Glucagon metabolism in man. Studies on the metabolic clearance rate and the plasma acute disappearance time of glucagon in normal and diabetic subjects. J. Clin. Endocrinol. Metab. 42, 830–838.
[5] Aronoff, S.L., Berkowitz, K., Shreiner, B. and Want, L. (2004) Glucose metabolism and regulation: beyond insulin and glucagon. Diabetes Spectr. 17, 183–190.
[6] Cryer, P.E. (1993) Glucose counterregulation: prevention and correction of hypoglycemia in humans. Am. J. Physiol. Endocrinol. Metab. 264, 149–155.
[7] Bosco, D., Armanet, M., Morel, P., Niclauss, N., Sgroi, A., Muller, Y.D., Giovannoni, L., Parnaud, G. and Berney, T. (2010) Unique arrangement of alpha- and beta-cells in human islets of Langerhans. Diabetes 59, 1202–1210.
[8] Cryer, P.E., Davis, S.N. and Shamoon, H. (2003) Hypoglycemia in diabetes. Diabetes Care 26, 1902–1912.
[9] Asplin, C.M., Paquette, T.L. and Palmer, J.P. (1981) *In vivo* inhibition of glucagon secretion by paracrine beta cell activity in man. J. Clin. Invest. 68, 314–318.
[10] Ben-Ami, H., Nagachandran, P., Mendelson, A. and Edoute, Y. (1999) Drug-induced hypoglycemic coma in 102 diabetic patients. Arch. Intern. Med. 159, 281–284.
[11] Bending, J.J., Pickup, J.C. and Keen, H. (1985) Frequency of diabetic ketoacidosis and hypoglycemic coma during treatment with continuous subcutaneous insulin infusion. Audit of medical care. Am. J. Med. 79, 685–691.
[12] Holleman, F., Schmitt, H., Rottiers, R., Rees, A., Symanowski, S. and Anderson, J.H.The Benelux-UK Insulin Lispro Study Group (1997) Reduced frequency of severe hypoglycemia and coma in well-controlled IDDM patients treated with insulin Lispro. Diabetes Care 20, 1827–1832.
[13] Raz, A. and Goodman, D.S. (1969) The interaction of thyroxine with human plasma prealbumin and with the prealbumin-retinol-binding protein complex. J. Biol. Chem. 244, 3230–3237.
[14] Maeda, S., Mita, S., Araki, S. and Shimada, K. (1986) Structure and expression of the mutant prealbumin gene associated with familial amyloidotic polyneuropathy. Mol. Biol. Med. 3, 329–338.
[15] Ando, Y. (2005) Liver transplantation and new therapeutic approaches for familial amyloidotic polyneuropathy (FAP). Med. Mol. Morphol. 38, 142–154.
[16] Weeke, B. and Jarnum, S. (1971) Serum concentration of 19 serum proteins in Crohn's disease and ulcerative colitis. Gut 12, 297–302.

[17] Ingenbleek, Y., De Visscher, M. and De Nayer, P. (1972) Measurement of prealbumin as index of protein-calorie malnutrition. Lancet 2, 106–109.
[18] Ingenbleek, Y. and Young, V.R. (2002) Transthyretin (prealbumin) in health and disease: nutritional implications. Annu. Rev. Nutr. 14, 495–533.
[19] Raguso, C.A., Genton, L., Dupertuis, Y.M. and Pichard, C. (2002) Assessment of nutritional status in organ transplant: is transthyretin a reliable indicator? Clin. Chem. Lab. Med. 40, 1325–1328.
[20] Aleshire, S.L., Bradley, C.A., Richardson, L.D. and Parl, F.F. (1983) Localization of human prealbumin in choroid plexus epithelium. J. Histochem. Cytochem. 31, 608–612.
[21] Cavallaro, T., Martone, R.L., Dwork, A.J., Schon, E.A. and Herbert, J. (1990) The retinal pigment epithelium is the unique site of transthyretin synthesis in the rat eye. Invest. Ophthalmol. Vis. Sci. 31, 497–501.
[22] Kawaji, T., Ando, Y., Nakamura, M., Yamamoto, K., Ando, E., Takano, A., Inomata, Y., Hirata, A. and Tanihara, H. (2005) Transthyretin synthesis in rabbit ciliary pigment epithelium. Exp. Eye Res. 81, 306–312.
[23] Jacobsson, B., Pettersson, T., Sandstedt, B. and Carlström, A. (1979) Prealbumin in the islets of Langerhans. IRCS Med. Sci. 7, 590.
[24] Westermark, G.T. and Westermark, P. (2008) Transthyretin and amyloid in the islets of Langerhans in type-2 diabetes. Exp. Diabetes Res. Article ID 429274.
[25] Itoh, N., Hanafusa, T., Miyagawa, J., Tamura, S., Inada, M., Kawata, S., Kono, N. and Tarui, S. (1992) Transthyretin (prealbumin) in the pancreas and sera of newly diagnosed type I (insulin-dependent) diabetic patients. J. Clin. Endocrinol. Metab. 74, 1372–1377.
[26] Tuitoek, P.J., Ziari, S., Tsin, A.T., Rajotte, R.V., Suh, M. and Basu, T.K. (1996) Streptozotocin-induced diabetes in rats is associated with impaired metabolic availability of vitamin A (retinol). Br. J. Nutr. 75, 615–622.
[27] Refai, E., Dekki, N., Yang, S.N., Imreh, G., Cabrera, O., Yu, L., Yang, G., Norgren, S., Rössner, S.M., Inverardi, L., Ricordi, C., Olivecrona, G., Andersson, M., Jörnvall, H., Berggren, P.O. and Juntti-Berggren, L. (2005) Transthyretin constitutes a functional component in pancreatic beta-cell stimulus-secretion coupling. Proc. Natl. Acad. Sci. USA 102, 17020–17025.
[28] Episkopou, V., Maeda, S., Nishiguchi, S., Shimada, K., Gaitanaris, G.A., Gottesman, M.E. and Robertson, E.J. (1993) Disruption of the transthyretin gene results in mice with depressed levels of plasma retinol and thyroid hormone. Proc. Natl. Acad. Sci. USA 90, 2375–2379.
[29] Cumming, G., Fidler, F. and Vaux, D.L. (2007) Error bars in experimental biology. J. Cell Biol. 177, 7–11.
[30] Cunnane, S., Nugent, S., Roy, M., Courchesne-Loyer, A., Croteau, E., Tremblay, S., Castellano, A., Pifferi, F., Bocti, C., Paquet, N., Begdouri, H., Bentourkia, M., Turcotte, E., Allard, M., Barberger-Gateau, P., Fulop, T. and Rapoport, S.I. (2011) Brain fuel metabolism, aging, and Alzheimer's disease. Nutrition 27, 3–20.
[31] Ando, Y., Yi, S., Nakagawa, T., Ikegawa, S., Hirota, M., Miyazaki, A. and Araki, S. (1991) Disturbed metabolism of glucose and related hormones in familial amyloidotic polyneuropathy: hypersensitivities of the autonomic nervous system and therapeutic prevention. J. Auton. Nerv. Syst. 35, 63–70.
[32] Jin, T. (2008) Mechanisms underlying proglucagon gene expression. J. Endocrinol. 198, 17–28.
[33] Huang, H.P. and Tsai, M.J. (2000) Transcription factors involved in pancreatic islet development. J. Biomed. Sci. 7, 27–34.
[34] Samadani, U., Qian, X. and Costa, R.H. (1996) Identification of a transthyretin enhancer site that selectively binds the hepatocyte nuclear factor-3 beta isoform. Gene Expr. 6, 23–33.
[35] Costa, R.H., Kalinichenko, V.V., Holterman, A.X. and Wang, X. (2003) Transcription factors in liver development, differentiation, and regeneration. Hepatology 38, 1331–1347.

PLOS ONE

A Pilot Investigation of Visceral Fat Adiposity and Gene Expression Profile in Peripheral Blood Cells

Masaya Yamaoka[1], Norikazu Maeda[1]*, Seiji Nakamura[2], Susumu Kashine[1], Yasuhiko Nakagawa[1], Aki Hiuge-Shimizu[1], Kohei Okita[1], Akihisa Imagawa[1], Yuji Matsuzawa[3], Ken-ichi Matsubara[2], Tohru Funahashi[1], Iichiro Shimomura[1]

1 Department of Metabolic Medicine, Graduate School of Medicine, Osaka University, Suita, Osaka, Japan, **2** DNA Chip Research Inc., Yokohama, Kanagawa, Japan, **3** Sumitomo Hospital, Osaka, Osaka, Japan

Abstract

Evidence suggests that visceral fat accumulation plays a central role in the development of metabolic syndrome. Excess visceral fat causes local chronic low-grade inflammation and dysregulation of adipocytokines, which contribute in the pathogenesis of the metabolic syndrome. These changes may affect the gene expression in peripheral blood cells. This study for the first time examined the association between visceral fat adiposity and gene expression profile in peripheral blood cells. The gene expression profile was analyzed in peripheral blood cells from 28 obese subjects by microarray analysis. Reverse transcription-polymerase chain reaction (RT-PCR) was performed using peripheral blood cells from 57 obese subjects. Obesity was defined as body mass index (BMI) greater than 25 kg/m^2 according to the Japanese criteria, and the estimated visceral fat area (eVFA) was measured by abdominal bioelectrical impedance. Analysis of gene expression profile was carried out with Agilent whole human genome 4×44 K oligo-DNA microarray. The expression of several genes related to circadian rhythm, inflammation, and oxidative stress correlated significantly with visceral fat accumulation. Period homolog 1 (PER1) mRNA level in blood cells correlated negatively with visceral fat adiposity. Stepwise multiple regression analysis identified eVFA as a significant determinant of PER1 expression. In conclusion, visceral fat adiposity correlated with the expression of genes related to circadian rhythm and inflammation in peripheral blood cells.

Citation: Yamaoka M, Maeda N, Nakamura S, Kashine S, Nakagawa Y, et al. (2012) A Pilot Investigation of Visceral Fat Adiposity and Gene Expression Profile in Peripheral Blood Cells. PLoS ONE 7(10): e47377. doi:10.1371/journal.pone.0047377

Editor: Reury F.P Bacurau, University of Sao Paulo, Brazil

Received May 14, 2012; **Accepted** September 11, 2012; **Published** October 16, 2012

Funding: This work was supported in part by Grants-in-Aid for Scientific Research (C) no. 22590979 (to N.M.) and Scientific Research on Innovative Areas no. 22126008 (to T.F.). The funders had no role in study design, data collection and analysis, decision to publish, or preparation of the manuscript.

Competing Interests: The authors have read the journal's policy and have the following conflicts: one or more of the authors are employed by a commercial company DNA Chip Research Inc. This does not alter the authors' adherence to all PLOS ONE policies on sharing data and materials.

* E-mail: norikazu_maeda@endmet.med.osaka-u.ac.jp

Introduction

It has been shown that there is a significant association between computed tomography (CT)-based fat distribution and life style-related diseases, such as diabetes, dyslipidemia, and hypertension. Visceral fat-related obesity is closely associated with the development of atherosclerotic diseases [1]. The metabolic syndrome is strongly linked to visceral fat adiposity. The exact pathomechanisms of the metabolic syndrome are not clear at present but seem to involve accumulation of macrophages in adipose tissue, which induce a state of chronic low-grade inflammation by producing a battery of inflammatory mediators. In addition, these macrophages interact with adipocytes through free fatty acids and adipocytokines, creating a vicious cycle that promotes the development of the metabolic syndrome and atherosclerosis [2–4]. However, to date, there is no method to evaluate the function and condition of human visceral fat.

A series of recent studies demonstrated that the adipose tissue of obese subjects contains not only macrophages but also non-macrophage immunocytes, such as T-cells [5,6], B-cells [7], and eosinophils [8], and that these cells accelerate the development of metabolic syndrome. These evidences imply that gene expression profile in peripheral blood cells may reflect the visceral fat condition. However, there is no report demonstrating the relation of peripheral blood gene expressions and visceral fat accumulation. Hence, the present study tested the association between visceral fat adiposity and the gene expression profile in peripheral blood cells to search novel surrogate markers relating to visceral fat adiposity and to establish novel diagnostic tools for metabolic syndrome.

Materials and Methods

Study Population

All subjects were inpatients of the Division of Endocrinology & Metabolism, Osaka University Hospital, Osaka. Written informed consent was obtained from each subject after explaining the purpose and potential complications of the study. The study protocol was approved by the human ethics committee of Osaka University and the study was registered with the University hospital Medical Information Network (Number: UMIN 000001663). Obesity was defined as body mass index (BMI) greater than 25 kg/m^2 [9]. Subjects with type 1 diabetes mellitus, autoimmune diseases, malignant diseases, and infectious diseases were excluded from the study. Patients treated with statins and/or thiazolidinediones were also excluded. Sixty-two subjects were

enrolled in the study, although five subjects were later excluded due to RNA degradation in the blood samples collected from these individuals. Thus, the present study was conducted in 57 obese patients.

Clinical Parameters

The estimated visceral fat area (eVFA) was measured by abdominal bioelectrical impedance analysis (BIA), as reported previously [10,11]. Physical examination and collection of blood samples were conducted on the same day. The homeostasis model−assessment of insulin resistance (HOMA-IR) was calculated by the equation: HOMA-IR = fasting insulin (μU/mL) x fasting glucose (mg/dL)/405.

The intima-media thickness (IMT) of the carotid arteries was measured using a high-resolution B-mode ultrasonography system (Xario; Toshiba Medical Systems Corp., Tochigi, Japan) with an electrical linear transducer (mid-frequency 7.5 MHz). IMT represented the distance between two parallel echogenic lines corresponding to the blood-intima and media-adventitia interfaces on the posterior wall of the artery. Three determinations of IMT were conducted at the site of the thickest point, maximum IMT (max-IMT) and two adjacent points (located 1 cm upstream and 1 cm downstream from this site). These three determinations were averaged and expressed as the mean IMT.

Type 2 diabetes mellitus was defined as fasting plasma glucose (FPG) concentration ≥126 mg/dL, 2-h plasma glucose concentration following 75 g oral glucose load of ≥200 mg/dL, or treatment with glucose-lowering agents. Hypertension was defined as systolic blood pressure (BP) ≥140 mmHg, diastolic BP≥90 mmHg, or treatment with anti-hypertensive agents. Dyslipidemia was defined as fasting triglycerides (TG) ≥150 mg/dL, high-density lipoprotein cholesterol (HDL-C) <40 mg/dL, or low-density lipoprotein cholesterol (LDL-C) ≥140 mg/dL, or treatment with lipid-lowering agents.

Isolation of RNA

For total RNA isolation, blood samples were collected into PaxGene Blood RNA tubes (PreAnalytiX/QIAGEN Inc., Valencia, CA) at 7:30 am and left to stand for 2 h at room temperature. The blood samples in the PaxGene Blood RNA tubes were stored at −20°C for 2 days and subsequently kept at −80°C until analysis. Total RNA was extracted by using PaxGene Blood RNA Kit (PreAnalytiX/QIAGEN) according to the protocol supplied by the manufacturer.

Microarray Analysis

After RNA was qualified by the Agilent 2100 Bioanalyzer, 250 ng of total RNA was converted to cDNA, amplified, and labeled with Cy3-labeled CTP using the Quick Amp Labeling kit (Agilent Technologies, Santa Clara, CA) according to the protocol supplied by the manufacturer. Following labeling and clean up, the amplified RNA and dye incorporation were quantified using a ND-1000 Spectrophotometer (Nano Drop Technologies, Wilmington, DE) and hybridized to Agilent whole human genome 4 × 44 K oligo-DNA microarray (Agilent Technologies, Santa Clara, CA). After hybridization, the arrays were washed consecutively by using Gene Expression Wash Pack (Agilent Technologies). Fluorescence images of the hybridized arrays were generated using the Agilent DNA Microarray Scanner, and the intensities were extracted with Agilent Feature Extraction software ver.10.7.3.1. The raw microarray data are deposited in the National Center for Biotechnology Information Gene Expression Omnibus (GEO Series GSE28038).

Real-Time RT-PCR

First-strand cDNA was synthesized from 180 ng of total RNA using Thermoscript RT (Invitrogen, Carlsbad, CA) and oligo dT primer. Real-time quantitative PCR amplification was conducted with the LightCycler 1.5 (Roche Diagnostics, Tokyo, Japan) using LightCycler-FastStart DNA Master SYBR Green I (Roche Diagnostics, Tokyo, Japan) according to the protocol recommended by the manufacturer. The final result for each sample was normalized to the respective GAPDH (glyceraldedyde-3-phosphate dehydrogenase) value. The primer sets used were: PER1, 5′-GAACTCAGATGTGGCTAGACC-3′ and 5′-TGTCAGCAACTTTGTCCAGGG-3′; GAPDH, 5′-AAGGGCATCCTGGGCTACA-3′ and 5′-GAGGAGTGGGTGTCGCTGTTG-3′.

Microarray Data Analyses

The raw microarray intensities were processed by the percentile shift method (75th percentile) using the GeneSpring GX11 (Agilent Technologies) so as to normalize the range of expression intensities for inter-microarray. Only those genes whose expression data were available in more than 50% of hybridizations were included for further analyses. The normalized data were exported from the GeneSpring GX software. The correlation between peripheral blood gene expression levels and Log-eVFA levels was examined by Pearson's correlation under the R environment (http://cran.at.r-project.org). Gene Ontology (GO) information was retrieved from the annotations in GeneSpring GX11.

Clinical Data Analysis

Geometric mean values were used for insulin and C-reactive protein (CRP) due to the skewed distribution of the data. Non-normally distributed variables were log-transformed before analysis. The Spearman rank correlation coefficients for the study population as a whole were analyzed for Log-eVFA levels and other clinical variables. A P values less than 0.05 denoted the presence of significant difference. Pearson's correlation coefficient was used to examine the relationship between period homolog 1 (PER1) and metabolic parameters. Stepwise multiple regression analysis with backward stepwise elimination was conducted to identify those parameters that significantly contributed to PER1. Log-eVFA, HOMA-IR, WBC and CRP were entered as independent variables in the analysis. All calculations were performed using the JMP software (JMP 9.0; SAS Institute Inc., Cary, NC). Data are expressed as mean±SD.

Results

Characteristics of the Subjects

The clinical characteristics of the participating subjects are listed in the Table 1. The mean BMI and eVFA of 57 patients were 30.6 kg/m^2 (range, 25.4–51.2 kg/m^2) and 166.8 cm^2 (range, 80–386 cm^2), respectively. The mean HOMA-IR was 3.0, reflecting mild insulin resistance. The proportion of patients with diabetes mellitus, dyslipidemia, and hypertension was 75%, 73%, and 57%, respectively. Frequency of patients treated with lipid-lowering drugs, anti-hypertensive drugs, oral glucose-lowering agents, insulin, and sleeping drugs was 25%, 42%, 18%, 42%, and 28%, respectively.

Serum adiponectin concentrations correlated inversely with eVFA (Figure S1A) while CRP levels correlated positively with eVFA (Figure S1B). Insulin concentrations correlated significantly with eVFA (Figure S1C) and HOMA-IR tended to increase in parallel with increase in eVFA (Figure S1D). The leukocyte count, but not the erythrocyte count or platelet count, correlated

Table 1. Characteristics of participants.

N	57
Age (years)	51.7±13.5
Male/Female	27.0/30
Body weight (kg)	79.4±16.7
BMI (kg/m^2)	30.6±5.3
Waist circumference (cm)	100.7±12.5
eVFA (cm^2)	166.8±164.4
Log-eVFA	2.2±0.15
Systolic blood pressure (mmHg)	128.8±14.9
Diastolic blood pressure (mmHg)	76.3±10.9
Fasting glucose (mg/dL)	139.6±50.3
Hemoglobin A1c (%)	8.1±2.2
Immunoreactive insulin (μU/ml)	12.1±5.8
HOMA-IR (unit)	3.0±1.3
Total cholesterol (mg/dL)	210.4±37.1
LDL-C (mg/dL)	134.1±33.3
HDL-C (mg/dL)	46.8±10.2
Triglyceride (mg/dL)	155.7±76.8
Creatinine (mg/dL)	0.8±0.29
Ureic acid (mg/dL)	6.2±1.5
Serum adiponectin (μg/mL)	6.7±4
WBC (/μL)	6758.0±1838
Neutrophils (%)	55.2±7.5
Lymphocytes (%)	35.8±8
Eosinophils (%)	3.0±1.5
Basophils (%)	0.6±0.9
Monocytes (%)	7.4±7.5
RBC (×10^4/μL)	466.0±53
Platelet (×10^4/μL)	23.4±5.6
CRP (mg/dL)	0.4±0.48
Diabetes mellitus, n (%)	43 (75)
Dyslipidemia, n (%)	42 (73)
Hypertention, n (%)	33 (57)
Mean IMT (mm)	0.9±0.25
Medication	
Oral glucose-lowering drugs, n (%)	10 (18)
Insulin, n (%)	24 (42)
Lipid lowering drugs, n (%)	14 (26)
Antihypertensive drugs, n (%)	24 (42)

Data are mean ± SD. BMI; body mass index, eVFA; estimated visceral fat area, LDL-C; low density lipoprotein-cholesterol, HDL-C; high density lipoprotein-cholesterol, HOMA-IR; homeostasis model assessment of insulin resistance, IMT; imtima-media thickness.

doi:10.1371/journal.pone.0047377.t001

significantly with eVFA (Figure S2A to S2C). Furthermore, the lymphocyte, monocyte, and neutrophil counts, but not those of eosinophils and basophils, correlated positively with eVFA (Figure S2D to S2H).

Analysis of Gene Expression Profiles

Peripheral blood RNA samples from 28 subjects (BMI 31.9±6.0 kg/m^2, VFA 199.4±89.4 cm^2) were subjected to microarray analysis. The target probes were selected under the condition that significant signals were detected in more than 14 cases and thus 27969 genes were extracted for gene expression analysis. Table 2 lists the top 20 genes that correlated significantly with eVFA: 8 genes correlated positively and 12 genes correlated negatively with eVFA. Among these genes, the solute carrier family 46 member 3 (SLC46A3), which is classified as a membrane protein, showed the highest statistical significance with eVFA ($P = 0.000006$). Importantly, significant correlations with eVFA were also observed in genes related to oxidative stress and inflammation, such as peroxiredoxin 3 (PRDX3) ($P = 0.00033$), suppressor of cytokine signaling 3 (SOCS3) ($P = 0.0007$), and ORAI calcium release-activated calcium modulator 1 (ORAI1) ($P = 0.0009$). Interestingly, a negative correlation with eVFA was observed in period homolog 1 (PER1), which is classified as a transcription factor and recognized as a circadian clock gene ($P = 0.0011$).

Next, we conducted gene ontology (GO) analysis and searched for genes involved in circadian rhythm (GO:0007623), inflammation (GO:0006954), oxidative stress (GO:0006979), immune response (GO:0006955), lipid metabolism (GO:0006629), and glucose metabolism (GO:0006006). Figure 1A shows the prevalence of genes that showed significant correlation with eVFA. The number of circadian rhythm genes was small, but 5 genes (18.5%) showed significant correlation with eVFA. The frequencies of inflammation-, oxidative stress-, and immune response-related genes that correlated significantly with eVFA were 5.9%, 7.8%, and 8.8%, respectively. Furthermore, the frequencies of lipid metabolism- and glucose metabolism-related genes that correlated

Table 2. Correlation coefficients of peripheral blood cell gene expression with visceral fat adiposity.

Gene Symbol	Gene Name	P value
Positively correlated genes		
SLC46A3	solute carrier family 46, member 3	0.000006
DUSP3	dual specificity phosphatase 3	0.00007
DEF8	differentially expressed in FDCP 8 homolog	0.0002
APOM	apolipoprotein M	0.00033
PRDX3	peroxiredoxin 3	0.00033
SOCS3	suppressor of cytokine signaling 3	0.0007
LOC644538	hypothetical protein LOC644538	0.0007
DOK4	docking protein 4	0.0011
Negatively correlated genes		
TSGA14	testis specific, 14	0.00002
CABIN1	calcineurin binding protein 1	0.00007
ZFP36	zinc finger protein 36	0.0001
RAB37	RAB37, member RAS oncogene family	0.0002
PBXIP1	pre-B-cell leukemia homeobox interacting protein 1	0.00032
RABGAP1L	RAB GTPase activating protein 1-like	0.0004
SMPD1	sphingomyelin phosphodiesterase 1, acid lysosomal	0.0004
ZNF174	zinc finger protein 174	0.0006
C3orf16	chromosome 3 open reading frame 16	0.0006
CCND3	cyclin D3	0.0007
ORAI1	ORAI calcium release-activated calcium modulator 1	0.0009
PER1	period homolog 1	0.0011

doi:10.1371/journal.pone.0047377.t002

significantly with eVFA were 3.0% and 6.1%, respectively. Increasing evidence demonstrates a close relationship between the disturbance of circadian clock oscillator and the development of metabolic syndrome [12–14]. Table 3 shows gene probes related to circadian rhythm (GO:0007623). PER1, v-erb-b2 erythroblastic leukemia viral oncogene homolog 3 (ERBB3), clock homolog (CLOCK), prokineticin 2 (PROK2), and cryptochrome 2 (CRY2) correlated significantly with eVFA.

Association between PER1 and Metabolic Parameters

As shown in Figure 1A and Table 3, genes relating to circadian rhythm were highly correlated with eVFA. The highest correlation with eVFA was observed in PER1 among them. RT-PCR was, therefore, performed in 57 subjects to revalue the association of eVFA and PER1 mRNA levels in peripheral blood cells. As shown in Figure 1B, PER1 mRNA levels correlated negatively with eVFA (Figure 1B).

Table 4 lists the correlation coefficients for the relationship between PER1 and various metabolic parameters. Age- and sex-adjusted univariate analysis showed that PER1 correlated negatively with log-eVFA, HOMA-IR, WBC, and CRP. Stepwise multiple regression analysis revealed log-eVFA as a significant determinant of PER1.

Discussion

The main findings of the present study were: *(1)* Visceral fat adiposity correlated with the expression of various genes related to circadian rhythm, inflammation, and oxidative stress, in peripheral blood cells. *(2)* Peripheral blood PER1 mRNA expression level correlated negatively with visceral fat area. *(3)* Visceral fat area

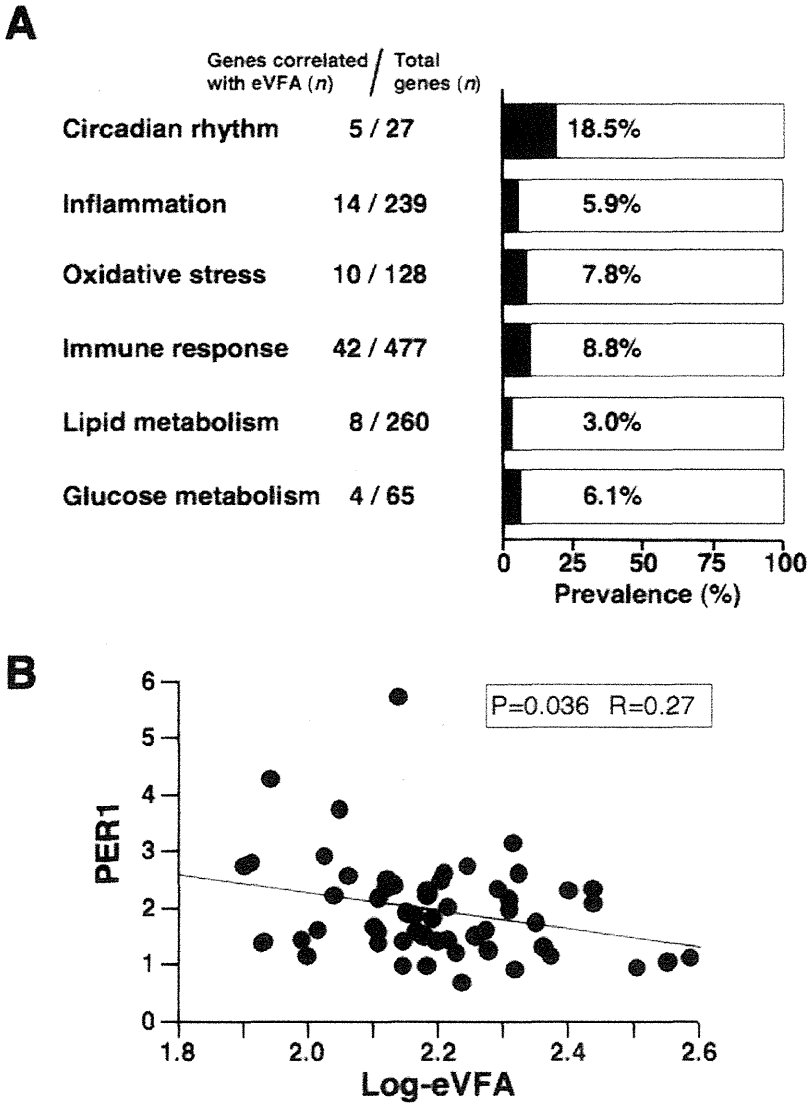

Figure 1. Gene expression profile in peripheral blood cells. (A) Prevalence of gene probes correlated with estimated visceral fat area (eVFA). Gene ontology analysis was performed based on the microarray data. (B) Correlation between PER1 mRNA level and eVFA. Total RNAs from peripheral blood cells of 57 subjects were subjected to RT-PCR.
doi:10.1371/journal.pone.0047377.g001

Table 3. Genes related to circadian rhythm.

Gene Symbol	Probe Name	P value
PER1	A_23_P89589	0.0011
ERBB3	A_23_P349416	0.0050
CLOCK	A_23_P419038	0.0120
PROK2	A_23_P97342	0.0230
CRY2	A_23_P127394	0.0489
CRY2	A_23_P388027	0.0565
CYP7B1	A_23_P169092	0.0669
CRY2	A_23_P158587	0.0699
AANAT	A_23_P152527	0.0704
CRY1	A_23_P36665	0.0864
PRF1	A_23_P1473	0.0939
HEBP1	A_23_P117082	0.0956
PHLPP1	A_23_P89762	0.1440
KCNMA1	A_23_P61150	0.1618
TIMELESS	A_23_P53276	0.2195
PER2	A_23_P411162	0.2494
PER2	A_23_P209320	0.3684
CRY1	A_24_P407235	0.4662
ATOH7	A_23_P378514	0.4755
ARNTL	A_24_P162037	0.5197
MAT2A	A_23_P401568	0.5893
NR1D1	A_23_P250227	0.7034
JUN	A_23_P420873	0.7405
HTR7	A_23_P500381	0.7585
MAT2A	A_32_P87703	0.9325
PROKR2	A_23_P412603	0.9702

PER1 : period homolog 1, ERBB3 : v-erb-b2 erythroblastic leukemia viral oncogene homolog 3, CLOCK : clock homolog, PROK2 : prokineticin 2, CRY2 : cryptochrome 2, CYP7B1 : cytochrome P450, family 7, subfamily B, polypeptide 1, ANNAT : arylalkylamine N-acetyltransferase, CRY1 : cryptochrome 1, PRF1 : *perforin 1, HEBP1 : heme binding protein 1, PHPP1 : PH domain and leucine rich* repeat protein phosphatase 1, KCNMA1 : potassium large conductance calcium-activated channel, subfamily M, alpha member 1, TIMELESS : timeless homolog, PER2 : Period homolog 2, ATOH7 : atonal homolog 7, ARNTL : aryl hydrocarbon receptor nuclear translocator-like, MAT2A : methionine adenosyltransferase II, alpha, NR1D1 : nuclear receptor subfamily 1, group D, member 1, JUN : jun oncogene, HTR7 : 5-hydroxytryptamine receptor 7, PROKR2 : prokineticin receptor 2.

doi:10.1371/journal.pone.0047377.t003

was a significant determinant of PER1 mRNA level in peripheral blood cells.

Chronic low-grade inflammation is closely associated with the metabolic syndrome. Immune cell infiltration and production of reactive oxygen species (ROS) are increased in obese adipose tissue and such changes can cause adipocyte dysfunction. The latter can cause disorders of circulating fatty acids, ROS, and adipocytokines, which are located upstream in the development of metabolic syndrome and atherosclerosis [5–8,15–17]. As shown in Table 2, several genes related to inflammation and ROS were associated with visceral fat adiposity, suggesting that inflammation of the adipose tissue may reflect on the expression of genes in peripheral blood cells. Interestingly, lymphocyte, monocyte, and neutrophil counts correlated positively with eVFA. The present data are in agreement with the reported increase in monocytes in obese subjects [18]. Such change in leukocyte subsets in visceral fat adiposity may be initiated by adipose local inflammation. Alternatively, it is also possible that the increase in the number of peripheral lymphocytes, monocytes, and neutrophils, which are somehow activated in bone marrow in visceral fat obesity, could results in the induction of local and/or systemic inflammation, with subsequent development of the metabolic syndrome. It is possible that some leukocyte subsets may affect the expression profile of certain genes, especially the mRNA level of PER1 in peripheral blood cells. PER1 mRNA level might be high in CD4-positive T cell rather than the other cells such as neutrophil, monocyte, CD8-positive T cell, and B cell, by analyzing microarray database (GSE22886)(data not shown), but further studies are needed to determine the exact leukocyte subtype(s) that influence peripheral blood PER1 mRNA level. In addition, target blood cell population of visceral fat should be identified in future.

Accumulating evidence indicates a close interrelationship between the circadian clock oscillator and metabolic syndrome [12–14]. Several genetic models of circadian disruption also exhibited metabolic disorders and vascular dysfunction [19]. One recent study highlighted the role of mouse Per genes in the development of obesity [20]. Furthermore, experimental evidence suggests that high-fat diet can alter the amplitude of peripheral circadian clock genes in mouse adipose tissue and liver [21]. In the present study, 18.5% of circadian genes in peripheral blood cells correlated significantly with eVFA (Figure 1A) and a significant correlation between PER1 mRNA level and eVFA was observed (Figure 1B). Other reports investigated circadian clock genes in human peripheral blood cells. In healthy male subjects, no distinct circadian changes were observed in the mRNA levels of PER2 and aryl hydrocarbon receptor nuclear translocator-like (ARNTL/BMAL1), whereas PER1 mRNA levels exhibited a clear oscillation during the 24-hour period with a peak expression level at 8 am [22]. We also obtained the preliminary data that the peripheral blood PER1 mRNA levels were oscillated with a peak expression level at 7:30 am (data not shown). These data support the present findings that peripheral blood PER1 mRNA level was reduced in visceral fat accumulation since the blood samples were collected exactly at 7:30 am in the present study. Circadian changes in Per1 mRNA were also reported in the mouse white adipose tissue [23] and disturbances of its expression were also reported in obese mice [24]. However, there is still a gap in our understanding of the circadian oscillation in mouse Per1 mRNA. Furthermore, the regulatory mechanism that control human PER1 expression in peripheral blood cells also remains uncertain. Haimovich et al [25] recently showed that a bolus administration of endotoxin resulted in down-regulation of PER1 mRNA in peripheral blood cells following a rise in plasma IL-6 and TNF-α levels but had no effect on melatonin secretory rhythm in human subjects [25]. Interestingly, our data (Table 4) showed that CRP was correlated with peripheral blood PER1 mRNA level. Considered collectively, it is possible that chronic low-grade inflammation could cause impairment of circadian oscillation of PER1 mRNA in peripheral blood cells with visceral fat accumulation. Alternatively, peripheral blood leukocytes with low PER1 mRNA level may have pro-inflammatory properties capable of initiating local inflammation in the adipose tissue. Further prospective studies are needed to examine whether dysregulation of circadian genes in peripheral blood cells can induce a vicious cycle, leading to the development of metabolic syndrome and cardiovascular events.

The present study has several limitations. Diabetes mellitus, dyslipidemia, and hypertension were common in the study population, since all subjects were inpatients. These metabolic diseases and medications could modulate the expression levels of various genes in peripheral blood cells directly or indirectly. The

Table 4. Correlation between PER1 and metabolic parameters.

	Univariate (non-adjusted)		Univariate (age,sex-adjusted)		Multivariate	
Parameter	**r**	**p value**	**R**	**p value**	**p value**	**F value**
Age	−0.28	0.031	-	-		
Sex	0.22	0.095	-	-		
BMI	−0.20	0.132	−0.27	0.047	-	-
Waist circumference (WC)	−0.26	0.044	−0.23	0.080		
Log-eVFA	−0.28	0.036	−0.29	0.023	0.005	8.969
Systolic blood pressure	−0.03	0.787	−0.03	0.786		
Diastolic blood pressure	0.05	0.705	−0.17	0.274		
Fasting glucose	−0.10	0.426	−0.12	0.354		
Hemoglobin A1c (JDS)	−0.17	0.206	−0.19	0.142		
HOMA-IR	−0.36	0.019	−0.42	0.013	0.090	3.074
AST	−0.13	0.329	−0.14	0.283		
ALT	−0.02	0.854	−0.10	0.439		
γ-GTP	−0.07	0.602	−0.08	0.551		
Total cholesterol	0.24	0.065	0.21	0.111		
LDL-C	0.19	0.149	0.17	0.202		
Triglyceride	0.10	0.456	−0.01	0.938		
HDL-C	0.11	0.389	0.20	0.128		
Creatinine	0.17	0.191	0.29	0.073		
Log adiponectin	−0.03	0.809	0.12	0.393		
WBC	−0.11	0.395	−0.37	0.011	0.087	3.128
CRP	−0.36	0.006	−0.37	0.003	0.096	2.968
Complication of DM		0.056	0.22	0.099		
Complication of HT		0.169	0.13	0.331		
Complication of DLP		0.788	0.02	0.885		
Mean IMT	0.02	0.886	0.10	0.551		

Data are mean ± SD. BMI; body mass index, eVFA; estimated visceral fat area, LDL-C; low density lipoprotein-cholesterol, HDL-C; high density lipoprotein-cholesterol, HOMA-IR; homeostasis model assessment of insulin resistance, DM; diabetes mellitus, HT; hypertension, DLP; dyslipidemia, IMT; imtima-media thickness.
doi:10.1371/journal.pone.0047377.t004

correlation between PER1 expression level and medication was also examined (data not shown), but there were no significant correlations in present study. Further studies will be needed in future to understand what kind of medications influence on peripheral blood cell mRNA expressions. In addition, the study participants were obese Japanese subjects (BMI $\geq$25 kg/m^2) and visceral fat area was measured by BIA, not CT or MRI. Future studies are needed to analyze the gene expression profile in peripheral blood cells from not only obese subjects but also non-obese healthy (low VFA) subjects, although we obtained the preliminary data that peripheral blood PER1 mRNA levels were significantly higher in non-obese healthy volunteers than in the current study population (data not shown). The effects of diet- and exercise-induced visceral fat reduction on gene expression profile in peripheral blood cells should be investigated in future.

In perspective, gene expression profiling in peripheral blood cells may be applied to detect the function and condition of visceral fat tissues in human, although further studies are needed in future. These analyses may provide the new knowledge of metabolic syndrome and will achieve the novel diagnostic and therapeutic approaches for metabolic syndrome.

Supporting Information

Figure S1 Correlation between estimated visceral fat area (eVFA) and various blood parameters. The homeostasis model−assessment of insulin resistance (HOMA-IR) was calculated as follows: HOMA-IR = fasting insulin (μU/mL)×fasting glucose (mg/dL)/405.
(TIFF)

Figure S2 Correlations between estimated visceral fat area (eVFA) and peripheral blood cell count.
(TIFF)

Acknowledgments

We thank Miyuki Nakamura, Department of Metabolic Medicine, Graduate School of Medicine, Osaka University, for the excellent technical assistance.

Author Contributions

Conceived and designed the experiments: NM YM KM TF IS. Performed the experiments: MY NM SN SK YN AHS KO AI. Analyzed the data: MY NM SN. Contributed reagents/materials/analysis tools: SN. Wrote the paper: NM MY SN.

References

1. Matsuzawa Y (2006) Therapy Insight: adipocytokines in metabolic syndrome and related cardiovascular disease. Nat Clin Pract Cardiovasc Med 3: 35–42.
2. Hotamisligil GS (2010) Endoplasmic reticulum stress and the inflammatory basis of metabolic disease. Cell 140: 900–917.
3. Flier JS (2004) Obesity wars: molecular progress confronts an expanding epidemic. Cell 116: 337–350.
4. Neels JG, Olefsky JM (2006) Inflamed fat: what starts the fire? J Clin Invest 116 : 33–35.
5. Feuerer M, Herrero L, Cipolletta D, Naaz A, Wong J, et al. (2009) Lean, but not obese, fat is enriched for a unique population of regulatory T cells that affect metabolic parameters. Nat Med 15: 930–939.
6. Nishimura S, Manabe I, Nagasaki M, Eto K, Yamashita H, et al.(2009) CD8+ effector T cells contribute to macrophage recruitment and adipose tissue inflammation in obesity. Nat Med 15: 914–920.
7. Winer DA, Winer S, Shen L, Wadia PP, Yantha J, et al. (2011) B cells promote insulin resistance through modulation of T cells and production of pathogenic IgG antibodies. Nat Med 17: 610–617.
8. Wu D, Molofsky AB, Liang HE, Ricardo-Gonzalez RR, Jouihan HA, et al. (2011) Eosinophils sustain adipose alternatively activated macrophages associated with glucose homeostasis. Science 332: 243–247.
9. Examination Committee of Criteria for 'Obesity Disease' in Japan (2002); Japan Society for the Study of Obesity. New criteria for 'obesity disease' in Japan. Circ J 66: 987–992.
10. Ryo M, Maeda K, Onda T, Katashima M, Okumiya A, et al. (2005) A new simple method for the measurement of visceral fat accumulation by bioelectrical impedance. Diabetes Care 28: 451–453.
11. Nakatsuji H, Kishida K, Funahashi T, Noguchi M, Ogawa T, et al. (2010) One-year reductions in body weight and blood pressure, but not in visceral fat accumulation and adiponectin, improve urinary albumin-to-creatinine ratio in middle-aged Japanese men. Diabetes Care 33: e110–111.
12. Bass J, Takahashi JS (2010) Circadian integration of metabolism and energetics. Science 330: 1349–1354.
13. Gimble JM, Sutton GM, Bunnell BA, Ptitsyn AA, Floyd ZE (2011) Prospective influences of circadian clocks in adipose tissue and metabolism. Nat Rev Endocrinol 7: 98–107.
14. Maury E, Ramsey KM, Bass J (2010) Circadian rhythms and metabolic syndrome: from experimental genetics to human disease. Circ Res 106: 447–462.
15. Weisberg SP, McCann D, Desai M, Rosenbaum M, Leibel RL, et al. (2003) Obesity is associated with macrophage accumulation in adipose tissue. J Clin Invest 112: 1796–1808.
16. Xu H, Barnes GT, Yang Q, Tan G, Yang D, et al. (2003) Chronic inflammation in fat plays a crucial role in the development of obesity-related insulin resistance. J Clin Invest 112 : 1821–1830.
17. Furukawa S, Fujita T, Shimabukuro M, Iwaki M, Yamada Y, et al. (2004) Increased oxidative stress in obesity and its impact on metabolic syndrome. J Clin Invest 114 : 1752–1761.
18. Kullo IJ, Hensrud DD, Allison TG (2002) Comparison of numbers of circulating blood monocytes in men grouped by body mass index (<25, 25 to <30, > or = 30). Am J Cardiol 89: 1441–1443.
19. Turek FW, Joshu C, Kohsaka A, Lin E, Ivanova G, et al. (2005) Obesity and metabolic syndrome in circadian Clock mutant mice. Science 308: 1043–1045.
20. Dallmann R, Weaver DR (2010) Altered body mass regulation in male mPeriod mutant mice on high-fat diet. Chronobiol Int 27: 1317–1328.
21. Kohsaka A, Laposky AD, Ramsey KM, Estrada C, Joshu C, et al. (2007) High-fat diet disrupts behavioral and molecular circadian rhythms in mice. Cell Metab 6: 414–421.
22. Fukuya H, Emoto N, Nonaka H, Yagita K, Okamura H, et al. (2007) Circadian expression of clock genes in human peripheral leukocytes. Biochem Biophys Res Commun 354: 924–928.
23. Zvonic S, Ptitsyn AA, Conrad SA, Scott LK, Floyd ZE, et al. (2006) Characterization of peripheral circadian clocks in adipose tissues. Diabetes 55: 962–970.
24. Ando H, Yanagihara H, Hayashi Y, Obi Y, Tsuruoka S, et al. (2005) Rhythmic messenger ribonucleic acid expression of clock genes and adipocytokines in mouse visceral adipose tissue. Endocrinology 146 : 5631–5636.
25. Haimovich B, Calvano J, Haimovich AD, Calvano SE, Coyle SM, et al. (2010) In vivo endotoxin synchronizes and suppresses clock gene expression in human peripheral blood leukocytes. Crit Care Med 38: 751–758.

INTERNAL MEDICINE

□ CASE REPORT □

Successful Treatment of Reactive Hypoglycemia Secondary to Late Dumping Syndrome Using Miglitol

Yukari Fujita[1], Daisuke Tamada[1], Junji Kozawa[1,2], Yoko Kobayashi[1], Shugo Sasaki[1], Tetsuhiro Kitamura[1], Tetsuyuki Yasuda[1], Norikazu Maeda[1], Michio Otsuki[1], Kohei Okita[1], Hiromi Iwahashi[1], Hideaki Kaneto[1], Tohru Funahashi[1,3], Akihisa Imagawa[1] and Iichiro Shimomura[1]

Abstract

We herein describe a 59-year-old woman who had undergone a total gastrectomy for gastric carcinoma and suffered from postprandial hypoglycemia characterized by a loss of consciousness and spasms. She was diagnosed with reactive hypoglycemia and treated with nutrition therapy, but the frequency and severity of the hypoglycemic episodes did not decrease. She was subsequently treated successfully with miglitol, an alpha-glucosidase inhibitor (α-GI) taken twice a day; other α-GIs (acarbose and voglibose) were not effective. In conclusion, the administration of miglitol was effective for preventing reactive hypoglycemia secondary to late dumping syndrome.

Key words: reactive hypoglycemia, dumping syndrome, alpha-glucosidase inhibitor

(Intern Med 51: 2581-2585, 2012)
(DOI: 10.2169/internalmedicine.51.8171)

Introduction

Reactive hypoglycemia is defined as a clinical disorder in which hypoglycemic symptoms occur postprandially. Serious and life-threatening hypoglycemia can occur without appropriate treatment (1, 2). Reactive hypoglycemia can be caused by fructose intolerance, galactosemia, drugs, and late dumping syndrome (3, 4). Late dumping syndrome is seen in 10-40% of patients after gastric surgery (5) and in more than 50% of patients after esophagectomy (6). In Japan, gastric cancer is one of the leading causes of cancer deaths (7), and gastrectomy is the mainstay of curative treatment (8).

Patients with reactive hypoglycemia secondary to late dumping syndrome are treated via dietary modifications, wherein meals are eaten five or six times a day, and the carbohydrate intake is reduced. However, this nutrition therapy is not always successful at preventing the development of hypoglycemia.

Alpha-glucosidase inhibitors (α-GIs), which are oral antidiabetic agents, work primarily in the small intestine. Because they reduce carbohydrate metabolism and carbohydrate absorption, they modulate the postprandial increase in the plasma glucose and insulin levels. Acarbose, an α-GI, has been reported to be effective in idiopathic reactive hypoglycemia (9, 10) and in late dumping syndrome (11, 12).

We herein report the case of a woman who suffered from severe reactive hypoglycemia secondary to late dumping syndrome and was successfully treated with miglitol twice a day, but for whom acarbose and voglibose were ineffective.

Case Report

A 59-year-old woman was admitted to Osaka University Hospital in September 2011 for the assessment and treatment of postprandial hypoglycemia. She had undergone total gastrectomy for gastric carcinoma in 2003. At that time, she was instructed to eat 6 divided small meals in a day, but she

[1]Department of Metabolic Medicine, Graduate School of Medicine, Osaka University, Japan, [2]Department of Community Medicine, Graduate School of Medicine, Osaka University, Japan and [3]Department of Metabolism and Atherosclerosis, Graduate School of Medicine, Osaka University, Japan

Received for publication May 15, 2012; Accepted for publication June 18, 2012

Correspondence to Dr. Junji Kozawa, kjunji@endmet.med.osaka-u.ac.jp

Table. Laboratory Data on Admission

	Patient		Reference	
WBC	3820	/μL	3300 - 9400	/μL
RBC	374 × 10^4	/μL	390 - 510 × 10^4	/μL
Hb	12.3	g/dL	12.0 - 15.0	g/dL
Plt	27.9 × 10^4	/μL	13 - 32 × 10^4	/μL
Na	141	mEq/L	139 - 146	mEq/L
K	4.2	mEq/L	3.6 - 4.8	mEq/L
Cl	105	mEq/L	100 - 108	mEq/L
AST	18	U/L	< 40	U/L
ALT	17	U/L	< 40	U/L
γGTP	28	U/L	12 - 69	U/L
LDH	168	U/L	103 - 229	U/L
ALP	258	U/L	134 - 359	U/L
UN	16	mg/dL	7 - 22	mg/dL
Cr	0.79	mg/dL	0.5 - 0.9	mg/dL
TP	6.3	g/dL	6.4 - 8.1	g/dL
Alb	3.6	g/dL	3.6 - 4.7	g/dL
T-Chol	195	mg/dL	150 - 220	mg/dL
TG	80	mg/dL	30 - 80	mg/dL
FPG	89	mg/dL	70 - 110	mg/dL
F-IRI	1.9	μU/mL	0 - 12	μU/mL
F-CPR	1.2	ng/mL	1.0 - 2.0	ng/mL
HbA1c (NGSP)	6.0	%	4.7 - 6.2	%
GAD Ab	2.8	U/mL	< 1.5	IU/L
Insulin Ab	< 0.4	%	< 0.4	%
TSH	5.74	μU/mL	0.40 – 3.80	μU/mL
FT4	0.8	ng/dL	0.9 – 1.6	ng/dL
FT3	2.4	pg/mL	2.0 – 3.4	pg/mL
TgAb	53.7	IU/mL	< 40	IU/mL
Cortisol	13.3	μg/dL	4.5 - 24.5	μg/dL
ACTH	23	pg/ml	< 60	pg/ml
GH	0.23	ng/mL	< 2.7	ng/mL
IGF-1	83.7	ng/ml	71 - 203	ng/ml
CEA	4	ng/mL	< 5	ng/mL
CA 19-9	12	U/mL	< 37	U/mL

WBC: white blood cells, RBC: red blood cells, Hb: hemoglobin, Plt: platelets, Na: sodium, K: potassium, Cl chlorine, AST: aspartate aminotransferase, ALT: alanine aminotransferase, γGTP: glutamyl transpeptidase, LDH, lactate dehydrogenase, ALP: alkaline phosphatase, UN, urea nitrogen, Cr: creatinine, TP: total protein, Alb: albumin, T Chol: total cholesterol, TG, triglyceride, FPG, fasting plasma glucose, F-IRI: fasting immunoreactive insulin, F-CPR: fasting C-peptide immunoreactivity, HbA1c, hemoglobin A1c, GAD Ab: glutamic acid decarboxylase antibody, Insulin Ab: insulin antibody, TSH: thyroid stimulating hormone, FT3: free triiodothyronine, FT4: free thyroxine, TgAb: thyroglobulin antibody, ACTH: adrenocorticotropic hormone, GH: growth hormone, IGF-1: insulin-like growth factor-1, CEA: carcinoembryonic antigen

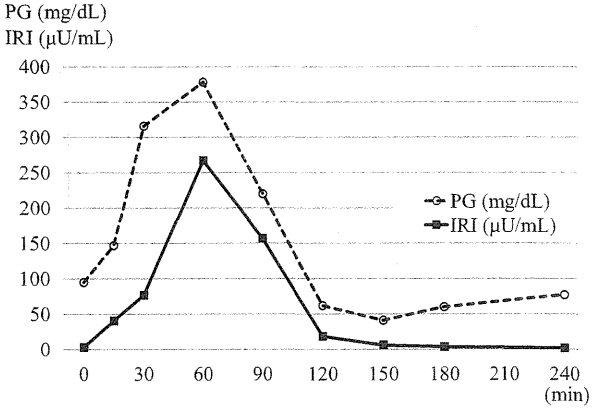

Figure 1. The results of the oral glucose tolerance test (75 g). The plasma glucose (○) and serum insulin (■) levels were measured up to 240 min after the glucose load.

frequently suffered from hypoglycemic episodes characterized by a loss of consciousness and spasms that occurred a few hours after meals. On two occasions, she was taken to an emergency room for hypoglycemic episodes; her plasma glucose level was 60 mg/dL on the first visit, in 2005, and 20 mg/dL on the second, in 2009. She had had no episodes of fasting hypoglycemia.

On admission in 2011, her height and weight were 152.4 cm and 45.9 kg (body mass index 19.9). Laboratory tests revealed mild glucose intolerance. The hemoglobin A1c (HbA1c) was estimated using the National Glycohemoglobin Standardization Program (NGSP) equivalent value (%) and calculated by the formula HbA1c (%) = HbA1c (Japan Diabetes Society [JDS], %) + 0.4%. Her HbA1c was 6.0%, and her fasting plasma glucose (FPG) level was 89 mg/dL. Her fasting immunoreactive insulin (F-IRI) and C-peptide immunoreactivity (F-CPR) were 1.9 μU/mL and 1.2 ng/mL, respectively. She was positive for anti-glutamic acid decarboxylase (GAD) antibodies. Although the anti-thyroglobulin antibody (TgAb) titer was also positive, her thyroid function was almost normal. Her adrenal function was also normal (Table).

An abdominal computed tomography (CT) scan detected no abnormalities in the pancreas. In a 75 g oral glucose tolerance test (OGTT), the baseline glucose and IRI levels were 95 mg/dL and 2.9 μU/mL, respectively; they rapidly increased to 378 mg/dL and 267.2 μU/mL after 60 minutes and decreased to 41 mg/dL and 5.9 μU/mL after 150 minutes (Fig. 1). Continuous glucose monitoring (CGMS-Gold™, Medtronic Minimed, Northridge, CA) under her regular diet revealed the mean blood glucose level to be 108 ± 52 mg/dL, and the blood glucose levels rapidly increased postprandially and then decreased to hypoglycemic levels after breakfast (Fig. 2A).

On the basis of these results, her hypoglycemia was diagnosed as reactive hypoglycemia secondary to late dumping syndrome. Every meal was divided into two, and the second meal was eaten 2 hours after the first. The total energy of the meals was 1,520 kcal/day. With the smaller, more frequent meals, the daily fluctuations in the blood glucose levels were reduced, and the mean blood glucose level was 108 ± 35 mg/dL. However, the reactive hypoglycemia following breakfast could not be prevented by dietary modifications alone (Fig. 2B). She was therefore given an additional α-GI orally, in combination with the dietary modifications. Because the postprandial hyperglycemia and hypoglycemia were most pronounced after breakfast in the hospital, an α-GI was administered once in the morning before the first

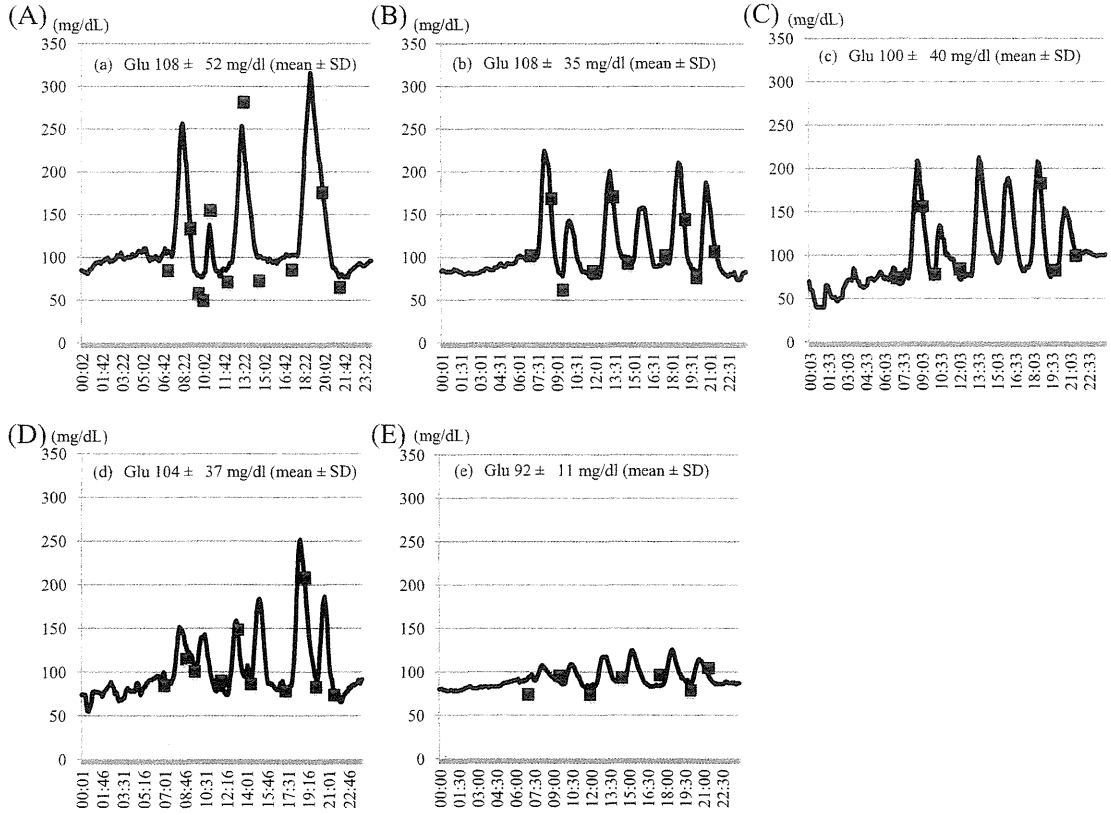

Figure 2. The daily profiles of the blood glucose levels according to CGMS under various conditions: (A) no medication, (B) divided meals, (C) after the addition of 0.3 mg of voglibose, (D) after the addition of 100 mg of acarbose and (E) after the addition of 50 mg of miglitol. Square symbols represent the self-monitored blood glucose levels.

meal. With the smaller, divided meals in combination with 0.3 mg of voglibose or 100 mg of acarbose, the mean blood glucose levels were 100 ± 40 mg/dL and 104 ± 37 mg/dL, respectively. Hence, these α-GIs were not effective for reducing the fluctuations of the blood glucose levels (Fig. 2C, D). However, after administration of 50 mg of miglitol, the mean blood glucose level was 92 ± 11 mg/dL, and the fluctuations throughout the day were markedly reduced (Fig. 2E).

The profiles of the blood glucose and IRI levels after breakfast (Fig. 3A, B) and after lunch (Fig. 3C, D) with the dietary modifications showed postprandial hyperglycemia and hyperinsulinemia, especially after breakfast. The administration of 0.3 mg of voglibose slightly reduced postprandial hyperinsulinemia following breakfast, but had no effect on the postprandial hyperglycemia after either breakfast or lunch. However, the administration of 50 mg of miglitol ameliorated both the postprandial hyperglycemia and the hyperinsulinemia, and the blood glucose level was elevated 120 minutes after breakfast, when reactive hypoglycemia often occurred.

Under a regimen of 50 mg of miglitol once a day, the peak plasma concentration (C_{max}) of miglitol was 2.2 μg/mL, the peak time (t_{max}) was 2.0 hours, and the half-life ($t_{1/2}$) was 2.8 hours. The amount of miglitol excreted in the urine was 28.5 mg/day, corresponding to 57% of the daily dose.

Under a regimen of 50 mg of miglitol once in the morning, the patient had infrequent hypoglycemic episodes after dinner in the hospital. Therefore, she was given an additional 50 mg of miglitol in the evening. After discharge, she was often constipated and was admitted to another hospital for a bowel obstruction, which was managed conservatively. Because her hypoglycemia is life-threatening, she has been carefully treated with the same dose of miglitol in conjunction with a laxative, and during the more than 6 months of follow-up, has not experienced any hypoglycemic episodes.

Discussion

We determined that miglitol, administered at 50 mg twice a day, was effective for preventing reactive hypoglycemia secondary to late dumping syndrome, and the efficacy of this agent was superior to that of two other α-GIs, voglibose and acarbose.

The differences in efficacy between these α-GIs might be attributable to their respective pharmacodynamics and pharmacokinetic properties. First, miglitol inhibits α-glucosidase in the upper section of the small intestine, which is the main site of intestinal absorption of glucose; almost all the miglitol is absorbed at this site (13, 14). In contrast, voglibose

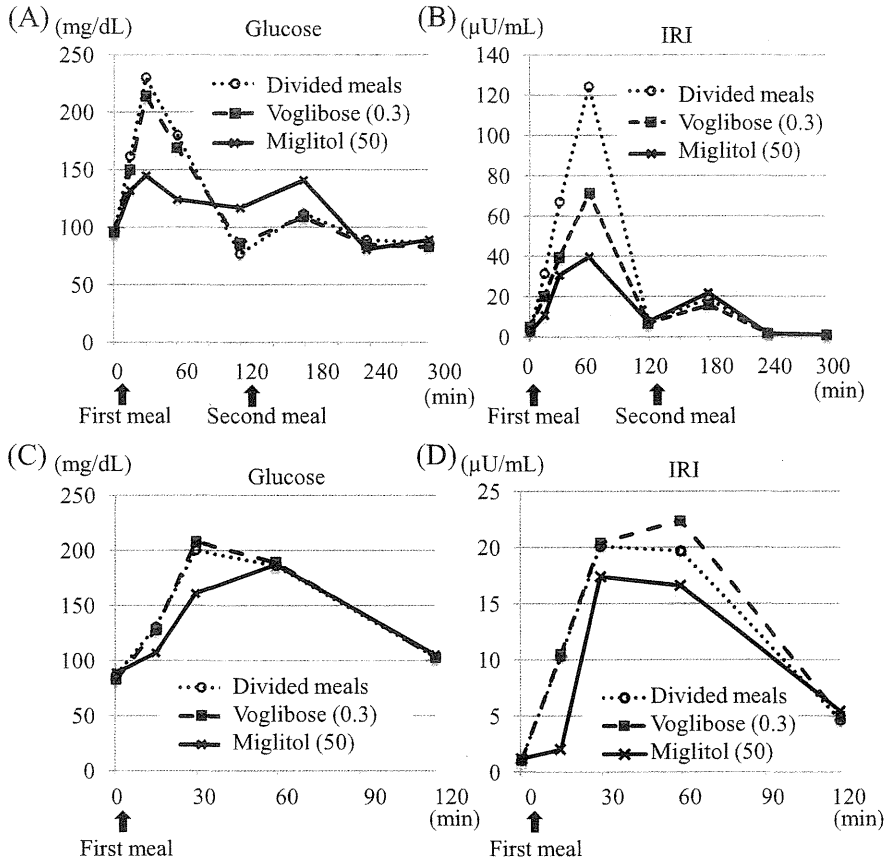

Figure 3. The profiles of the blood glucose and IRI levels (A, B) after breakfast and (C, D) after lunch with divided meals (○), after the addition of 0.3 mg of voglibose (■) or after the addition of 50 mg of miglitol (X).

and acarbose are not absorbed, and thus inhibit α-glucosidase throughout the small intestine. Second, miglitol has different specificities and affinities for the various metabolic enzymes compared with voglibose and acarbose (15). While acarbose is a complex oligosaccharide, miglitol is structurally similar to glucose; this similarity is suggested to be related to its broader specificity of inhibition against α-glucosidases (13). The inhibition of α-glucosidase primarily in the upper section of the small intestine and the broader specificity may lead to a significant advantage for miglitol in reducing the rapid postprandial increase of blood glucose and IRI levels compared with other α-GIs in patients with reactive hypoglycemia secondary to dumping syndrome, as has been reported in patients with type 2 diabetes (16-18).

The saturated absorption of miglitol in the upper section of the small intestine may be one mechanism through which the twice-daily administration of 50 mg of miglitol could prevent postprandial hyperglycemia and the reactive hypoglycemia throughout the day. At this site, the absorption of miglitol is already saturated, as has been reported for Caucasians, within the therapeutic dose range (with doses ≥50 mg or ≥0.7 mg/kg), and miglitol is not readily absorbed in the ileum or colon (14). For our patient, the administration 50 mg of miglitol corresponded to 1.1 mg/kg of miglitol. The unabsorbed miglitol may inhibit α-glucosidase for a longer period of time in the lower sections of the small intestine or colon. Indeed, when she was administered 50 mg of miglitol once a day, the daily amount of excretion of miglitol via urine corresponded to approximately 60% of the daily dose, thus suggesting that 40% could not be absorbed.

Another possible mechanism may be related to a change in incretin secretion. Miglitol enhances postprandial secretion of glucagon-like peptide-1 (GLP-1) (19-24), a gut peptide secreted by intestinal L cells in response to nutrient ingestion. In addition, the administration of miglitol once in the morning induced a prolonged increase of GLP-1 secretion not only after breakfast, but also after lunch, in non-diabetic men (19) and in patients treated with sitagliptin for type 2 diabetes (20). GLP-1 has a physiological effect of inhibiting gastrointestinal motility, including the slowing of gastric emptying (25, 26). An increased release of GLP-1 following the administration of miglitol may cause a decrease in gastrointestinal motility. In our patient who had undergone a total gastrectomy, the decreased gastrointestinal motility other than gastric emptying might have led to a reduction in the rapid postprandial increase in the glucose and insulin levels, which are the main causes of reactive hypoglycemia secondary to late dumping syndrome. In this case, the C_{max} of miglitol was much higher, and the $t_{1/2}$ was slightly longer than that in healthy volunteers who were ad-

ministered 1.4 mg/kg of miglitol (C_{max}; 1.13 μg/mL, $t_{1/2}$; 2.35 hours), while the duration of time at the t_{max} was not longer (2.0 hours in this case v.s. 2.3 hours in healthy volunteers) (14). It has been speculated that gastric surgery may induce augmented GLP-1 secretion and retention of miglitol in the upper section of the small intestine, while the absence of the stomach may allow miglitol to more rapidly reach the upper section of small intestine, thus leading to almost the same t_{max}. Therefore, the increased and prolonged release of GLP-1 resulting from twice-daily administration of miglitol may have contributed to the prevention of reactive hypoglycemia throughout the day. However, the secretion of miglitol-induced incretin, in addition to abdominal surgery, may reduce gastrointestinal motility and thus lead to bowel obstruction, as occurred in this case. The blood incretin concentrations and the rate of gastrointestinal motility were not examined in this patient. Therefore, further studies are needed to investigate this hypothesis.

In conclusion, the administration of miglitol, but not other α-GIs, twice a day was effective for preventing reactive hypoglycemia secondary to late dumping syndrome in our patient.

The authors state that they have no Conflict of Interest (COI).

Acknowledgement

This work received support from Sanwa Kagaku Kenkyusho, Co. Ltd., Japan, for the pharmacokinetic analysis of miglitol.

Yukari Fujita and Daisuke Tamada contributed equally to this work.

References

1. Bellini F, Sammicheli L, Ianni L, Pupilli C, Serio M, Mannelli M. Hypoglycemia unawareness in a patient with dumping syndrome: report of a case. J Endocrinol Invest **21**: 463-467, 1998.
2. Teno S, Nakajima-Uto Y, Nagai K, et al. Treatment with alpha-glucosidase inhibitor for severe reactive hypoglycemia: a case report. Endocr J **47**: 437-442, 2000.
3. Marks V, Teale JD. Hypoglycaemia in the adult. Baillières Clin Endocrinol Metab **7**: 705-729, 1993.
4. Gilbert JA, Dunlop DM. Hypoglycaemia following partial gastrectomy. Br Med J **30**: 330-332, 1947.
5. Vecht J, Masclee AA, Lamers CB. The dumping syndrome. Current insights into pathophysiology, diagnosis and treatment. Scand J Gastroenterol **223**(Suppl): 21-27, 1997.
6. McLarty AJ, Deschamps C, Trastek VF, Allen MS, Pairolero PC, Harmsen W. Esophageal resection for cancer of the esoph-agus: Long-term function and quality of life. Ann Thorac Surg **67**: 1568-1572, 1997.
7. Hamashima C, Shibuya D, Yamazaki H, et al. The Japanese guidelines for gastric cancer screening. Jpn J Clin Oncol **38**: 259-267, 2008.
8. Makoto Saka, Shinji Morita, Takeo Fukagawa, Hitoshi Katai. Present and future status of gastric cancer surgery. Jpn J Clin Oncol **41**: 307-313, 2011.
9. Peter S. Acarbose and idiopathic reactive hypoglycemia. Horm Res **60**: 166-167, 2003.
10. Tamura Y, Araki A, Chiba Y, Horiuchi T, Mori S, Hosoi T. Postprandial reactive hypoglycemia in an oldest-old patient effectively treated with low-dose acarbose. Endocr J **53**: 767-771, 2006.
11. Hasegawa T, Yoneda M, Nakamura K, et al. Long-term effect of alpha-glucosidase inhibitor on late dumping syndrome. J Gastroenterol Hepatol **13**: 1201-1206, 1998.
12. Teno S, Nakajima-Uto Y, Nagai K, et al. Treatment with alpha-glucosidase inhibitor for severe reactive hypoglycemia: a case report. Endocr J **43**: 511-516, 1996.
13. Scott LJ, Spencer CM. Miglitol: a review of its therapeutic potential in type 2 diabetes mellitus. Drugs **59**: 521-549, 2000.
14. Ahr AJ, Boberg M, Brendel E, Krause HP, Steinke W. Pharmacokinetics of miglitol. Absorption, distribution, metabolism, and excretion following administration to rat, dogs, and man. Arzneimittelforschung **47**: 734-745, 1997.
15. Samulitis BK, Goda T, Lee SM, Koldovský O. Inhibitory mechanism of acarbose and 1-deoxynojirimycin derivatives on carbohydrases in rat small intestine. Drugs Exp Clin Res **13**: 517-524, 1987.
16. Hiki M, Shimada K, Kiyanagi T, et al. Single administration of alpha-glucosidase inhibitors on endothelial function and incretin secretion in diabetic patients with coronary artery disease-Juntendo University trial: effects of miglitol on endothelial vascular reactivity in type 2 diabetic patients with coronary heart disease (J-MACH)-. Circ J **74**: 1471-1478, 2010.
17. Tsujino D, Nishimura R, Taki K, Morimoto A, Tajima N, Utsunomiya K. Comparison the efficacy of α-glucosidase inhibitors in suppressing postprandial hyperglycemia using continuous glucose monitoring: a pilot study-the MAJOR study. Diabetes Technol Ther **12**: 379-381, 2011.
18. Narita T, Yokoyama H, Yamashita R, et al. Comparison of the effects of 12-week administration of miglitol and voglibose on the responses of plasma incretins after a mixed meal in Japanese type 2 diabetic patients. Diabetes Obes Metab 2011, DOI: 10.1111/j.1463-1326.2011.01526.x.
19. Masuda K, Aoki K, Terauchi Y. Effects of miglitol taken just before or after breakfast on plasma glucose, serum insulin, glucagon and incretin levels after lunch in men with normal glucose tolerance, impaired fasting glucose or impaired glucose tolerance. J Diabet Invest **2**: 435-440, 2011.
20. Aoki K, Kamiyama H, Yoshimura K, Shibuya M, Masuda K, Terauchi Y. Miglitol administered before breakfast increased plasma active glucagon-like peptide-1 (GLP-1) levels after lunch in patients with type 2 diabetes treated with sitagliptin. Acta Diabetol, DOI: 10.1007/s00592-011-0322-9
21. Narita T, Katsuura Y, Sato T, et al. Miglitol induces prolonged and enhanced glucagon-like peptide-1 and reduced gastric inhibitory polypeptide response after ingestion of a mixed meal in Japanese type 2 diabetic patients. Diabet Med **26**: 187-188, 2009.
22. Arakawa M, Ebato C, Mita T, et al. Miglitol suppresses the postprandial increases in interleukin 6 and enhances active glucagon-like peptide 1 secretion in viscerally obese subjects. Metabolism **57**: 1299-1306, 2008.
23. Lee A, Patrick P, Wishart J, Horowitz M, Morley JE. The effects of miglitol on glucagon-like peptide-1 secretion and appetite sensations in obese type 2 diabetics. Diabetes Obes Metab **4**: 329-335, 2002.
24. Aoki K, Miyazaki T, Nagakura J, Orime K, Togashi Y, Terauchi Y. Effects of pre-meal versus post-meal administration of miglitol on plasma glucagon-like peptide-1 and glucose dependent insulinotropic polypeptide levels in healthy men. Endocr J **57**: 673-677, 2010.
25. Nauck MA, Kemmeries G, Holst JJ, Meier JJ. Rapid tachyphylaxis of the glucagon-like peptide 1-induced deceleration of gastric emptying in humans. Diabetes **60**: 1561-1565, 2011.
26. Holst JJ, Deacon CF, Visvll T, Krarup T, Madsbad S. Glucagon-like peptide-1, glucose homeostasis and diabetes. Trends Mol Med **14**: 161-168, 2008.

Fujishima et al. Cardiovascular Diabetology 2012, 11:107
http://www.cardiab.com/content/11/1/107

CARDIO VASCULAR DIABETOLOGY

ORIGINAL INVESTIGATION Open Access

Efficacy of liraglutide, a glucagon-like peptide-1 (GLP-1) analogue, on body weight, eating behavior, and glycemic control, in Japanese obese type 2 diabetes

Yuya Fujishima, Norikazu Maeda*, Kana Inoue, Susumu Kashine, Hitoshi Nishizawa, Ayumu Hirata, Junji Kozawa, Tetsuyuki Yasuda, Kohei Okita, Akihisa Imagawa, Tohru Funahashi and Iichiro Shimomura

Abstract

Background: We recently reported that short-term treatment with liraglutide (20.0 ± 6.4 days) reduced body weight and improved some scales of eating behavior in Japanese type 2 diabetes inpatients. However, it remained uncertain whether such liraglutide-induced improvement is maintained after discharge from the hospital. The aim of the present study was to determine the long-term effects of liraglutide on body weight, glycemic control, and eating behavior in Japanese obese type 2 diabetics.

Methods: Patients with obesity (body mass index (BMI) >25 kg/m^2) and type 2 diabetes were hospitalized at Osaka University Hospital between November 2010 and December 2011. BMI and glycated hemoglobin (HbA1c) were examined on admission, at discharge and at 1, 3, and 6 months after discharge. For the liraglutide group (BMI; 31.3 ± 5.3 kg/m^2, n = 29), patients were introduced to liraglutide after correction of hyperglycemic by insulin or oral glucose-lowering drugs and maintained on liraglutide after discharge. Eating behavior was assessed in patients treated with liraglutide using The Guideline For Obesity questionnaire issued by the Japan Society for the Study of Obesity, at admission, discharge, 3 and 6 months after discharge. For the insulin group (BMI; 29.1 ± 3.0 kg/m^2, n = 28), each patient was treated with insulin during hospitalization and glycemic control maintained by insulin after discharge.

Results: Liraglutide induced significant and persistent weight loss from admission up to 6 months after discharge, while no change in body weight after discharge was noted in the insulin group. Liraglutide produced significant improvements in all major scores of eating behavior questionnaire items and such effect was maintained at 6 months after discharge. Weight loss correlated significantly with the decrease in scores for recognition of weight and constitution, sense of hunger, and eating style.

Conclusion: Liraglutide produced meaningful long-term weight loss and significantly improved eating behavior in obese Japanese patients with type 2 diabetes.

Keywords: Liraglutide, Glucagon-like peptide-1 (GLP-1), Obesity, Eating behavior, Diabetes, Incretin

* Correspondence: norikazu_maeda@endmet.med.osaka-u.ac.jp
Department of Metabolic Medicine, Graduate School of Medicine, Osaka University, 2-2-B5, Yamada-oka, Suita, Osaka 565-0871, Japan